ACS OMEGA

Open Access

http://pubs.acs.org/journal/acsodf

Article

Oral Release Kinetics, Biodistribution, and Excretion of Dopants from Barium-Containing Bioactive Glass in Rats

Shreyasi Majumdar, Anshul Tiwari, Debasmit Mallick, Devendra K. Patel, Surendra Kumar Trigun, and Sairam Krishnamurthy*

Cite This: *ACS Omega* 2024, 9, 7188−7205

Read Online

ACCESS | Metrics & More | Article Recommendations | Supporting Information

ABSTRACT: *Background*: Inorganic biomaterials are biologically active and are used as implants and drug delivery system. They have therapeutically active elements present in their framework that are released in the physiological milieu. Release of these dopants above the supraphysiological limit may produce adverse effects and physicochemical interactions with the loaded drugs. Therefore, this necessitates evaluating the *in vivo* release kinetics, biodistribution, and excretion profiles of dopants from barium-doped bioglass (BaBG) that has potential anti-inflammatory, antiulcer, and regenerative properties. *Methods*: *In vitro* leaching of Ca, Si, and Ba from BaBG was analyzed in simulated body fluid. Release kinetics post single-dose oral administration (1, 5, and 10 mg/kg) was performed in rats. Blood was collected at different time points, and pharmacokinetic parameters of released elements were calculated. The routes of excretion and biodistribution in major organs were evaluated using ICP-MS. *Results*: Elements were released after the oral administration of BaBG into the plasma. They showed dose-dependent release kinetics and mean residence time. C_{max} was observed at 24 h for all elements, followed by a downhill fall. There was also a dose-dependent increase in the volume of distribution, and the clearance of dopants was mostly through feces. Ba and Si were biodistributed significantly in the liver, spleen, and kidneys. However, by the end of day 7, there was a leveling-off effect observed for all elements. *Conclusion*: All of the dopants exhibited a dose-dependent increase in release kinetics and biodistribution in vital organs. This study will help in dose optimization and understanding of various physicochemical and pharmacokinetic interactions when BaBG is used for future pharmacological studies.

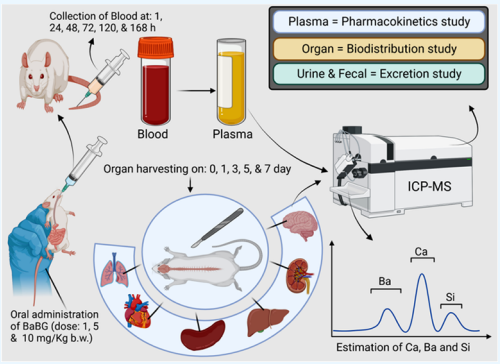

1. INTRODUCTION

Bioactive glasses (BGs) are bio- and cytocompatible third-generation silica-based inorganic compounds that have tremendous tissue regenerative potential.[1] Their bioactivity is mainly due to various therapeutic dopants present in its silica network that are leached into the physiological environment,[2,3] which activates a cascade of proteins or ion channels required for physiological activity. Preclinically, BGs have been reported to possess several biological effects and are used topically as a hemostatic agent for wound healing.[1,3] They also facilitate neovascularization[4] and are used as cardiac patches to prevent anoikis.[5] Besides, the pharmacological efficacy of BGs has also been explored and the orally administered barium-doped BG (BaBG) exhibited an antiulcer effect in various gastric ulcer models in rats.[6] Inorganic pharmaceuticals are even used in modern clinical medicines for the treatment of neurological disorders or as supplements.[7] Therefore, the clinical translation of BGs for systemic use necessitates investigating the release kinetic profile and biodistribution of the dopants leached from BGs that are designed for therapeutic applications. In addition, BGs are also preferred as a multifunctional delivery system owing to their tailorable topographical features that favor the entrapment and delivery of a multitude of therapeutics.[8] Further, due to the inherent osteogenic and bactericidal properties, BGs are also used clinically as orthopedic implants for extremely serious orthopedic deformities.[9,10] The clinical implants for osseous tissues are required to be present *in situ* throughout the patient's life. So, these implants must have higher stability with low leaching tendency. Hence, determining the preclinical release kinetic profile of the dopants of BGs will shed light on their chemical and biological stability when used as implants.

In general, the therapeutic ions that are doped in the silica network of BGs are an integral part of the normal physiology of body where the ionic homeostasis is maintained.[3] These physiologically and pharmacologically active dopants produce therapeutic efficacy if the leaching ionic concentrations are within physiological limits. However, if this physiological ionic set-point is broken due to excessive leaching of doped

Received: November 20, 2023
Revised: January 13, 2024
Accepted: January 18, 2024
Published: January 31, 2024

elements, it may lead to various physicochemical, pharmacokinetic, and pharmacodynamic interactions.[11,12] Additionally, the release of dopants from BGs causes an increase in the pH, which may alter the bioavailability of weak acidic drugs whose absorption is pH-dependent[13] and hence may affect their onset of action and bioavailability. Moreover, BGs may even cause increased accumulation of dopants in excretory organs, which will change the *in situ* ionic homeostasis.[14] This may alter the excretion of drugs that may remain in the body, even after their normal washout periods. Hence, this makes it necessary to perform biodistribution and excretion of the leached elements before using them as a drug carrier.

Further, understanding the fate of the dopants released after oral administration is highly important for optimizing the dose regimens, which can be determined from the *in vivo* pharmacokinetic study.[15] It will also help in determining the absorption, tissue distribution, metabolism, and excretion of the released dopants. Moreover, since the kinetic profile of the dopants indirectly determines their residence time in the body, it can also be used to predict the potential adverse effects that they might produce if used for a longer duration.[15] The clinical translation of inorganic nanomaterials demands controlled elimination with minimum organ accumulation. Hence, this is the first investigational preclinical study performed to explore the release kinetics of therapeutic ions leached from BG, their pharmacokinetic parameters, biodistribution, and excretion when administered orally in rats. Administration of drugs *via* the oral route is preferred clinically because of patient compliance, and performing oral pharmacokinetic and biodistribution studies will help to elucidate the effects of gastric contents and food on release kinetics.

45S5 (Bioglass), the parent inorganic biomimetic BGs, has a silicate framework with calcium ions present as a network modifier.[1,16] Following this, several therapeutic ions have been doped in the BG framework, which imparts enhanced pharmacological activity and therapeutic efficacy.[3,8] One such trace nonessential element for the human body is barium, reported to be involved in the calcification of the skeletal system.[17,18] Further, barium salts are also used as diagnostic radiocontrast agents[19] and have several biological properties.[3,20,21] Therefore, barium was doped into the bioglass framework (BaBG) and exhibited antiulcer properties in rats.[6] Notably, BaBG has also been shown to possess *in vitro* regeneration potential in addition to the anti-inflammatory properties[20] in LPS-induced neuroinflammation. BaBG is safer and devoid of any organ toxicity, with a lethal dose (LD_{50}) of more than 2000 mg/kg b.w.[22] Thus, BaBG has the potential to be used as a regenerative medicine in various disease models.

Therefore, in the present study, the sol−gel-derived BaBG was characterized to affirm its inherent amorphous phase using XRD and its *in vitro* hydroxyapatite (HA) forming ability using various spectroscopic techniques (FTIR), scanning electron microscopy (SEM), and elemental analysis (EDX). Similarly, the *in vitro* release kinetics of various dopants from BaBG in SBF and the alteration in pH of the solution were also accessed. Further, the changes in plasma concentration of Ca, Ba, and Si after single-dose oral administration of BaBG were studied in rats at various time points using inductively coupled plasma mass spectrometer (ICP-MS), and the pharmacokinetic parameters were calculated using PK Solver. The distribution of therapeutic dopants from BaBG in various organs and their route of excretion were investigated in urine and feces. In addition, the SEM study of the tissue sections of the brain, heart, lungs, liver, kidneys, and spleen of the BaBG-treated rats was performed to analyze the topographical and surface morphological changes in the organs post BaBG treatment.

2. MATERIALS AND METHODS

2.1. Materials. Nitric acid, perchloric acid, acetone, and tetraethyl orthosilicate (TEOS) were procured from Sigma-Aldrich. Triethyl phosphate (TEP), calcium nitrate tetrahydrate, sodium nitrate, and barium nitrate were purchased from Merck. Carboxymethyl cellulose (CMC), paraformaldehyde, glutaraldehyde, and chemicals used to prepare phosphate buffer solution were obtained from SRL, India.

2.2. Preparation of BaBG Using Sol−Gel Method. BaBG ($44.85SiO_2-2.6P_2O_5-24.3Na_2O-26.9CaO-1.35BaO$ mol %) was synthesized by the sol−gel method as previously reported[20] using analytical grade chemicals. Briefly, the precursors of SiO_2, P_2O_5, Cao, Na_2O, and BaO (TEOS, TEP, calcium nitrate tetrahydrate, sodium nitrate, and barium nitrate, respectively) were weighted and stirred thoroughly in an ethanol/water mixture containing diluted nitric acid solution for homogeneous mixing followed by aging of the gel formed. Then, the aged gel was dried in an oven to remove excess water and stabilized thermally at 550 °C in an oxidizing environment. Fine-powered BaBG was obtained by pulverization in a planetary ball mill (VB Ceramics, India).

2.3. Preparation of Simulated Body Fluid (SBF). The *in vitro* leaching of doped elements from the BG samples was carried out in the SBF that has an ionic concentration comparable to human plasma.[23] Na^+, $HCO3^-$, K^+, Cl^-, HPO_4^{2-}, Mg^{2+}, Ca^{2+}, and SO_4^{2-} present in SBF were obtained from NaCl, $NaHCO_3$, KCl, K_2HPO_4, $MgCl_2$, $CaCl_2$, and Na_2SO_4, respectively. All of the ingredients were dissolved in distilled water at 37 °C, and the pH was adjusted to 7.4.

2.4. Characterization of the Synthesized BaBG and Apatite Formation Assessment. The surface area, pore size, and diameter of the BaBG were analyzed by the Brunauer−Emmett−Teller (BET) and Barrett−Joyner−Halenda (BJH) methods during nitrogen adsorption−desorption measurements (Quantachrome Instruments NOVA 1000).[24] The mean diameter of synthesized BaBG was determined using a particle size analyzer as previously reported.[22] Further, BaBG after incubation with SBF for 7 days was filtered followed by washing with deionized water and oven-dried at 60 °C for 5 h. The formation of an HA layer was affirmed by Fourier transform infrared (FTIR) spectroscopy, X-ray diffraction (XRD), and SEM−EDX. The phase analysis of BaBG before and after treatment with SBF was determined by XRD (RIGAKU-Miniflex II diffractometer) at 2θ, varying from 20 to 80° with a step size of 0.02°, and the interpretation of peak was validated by utilizing the standard JCPDS-International Centre for Diffraction Data Cards. Similarly, the functional group present in BaBG and the newly formed HCA post SBF treatment were characterized by FTIR (FTIR-8400S, SHIMADZU). The surface morphology and changes in the elemental composition were evaluated by SEM−EDX (EVO/18 Research, ZEISS).

2.5. Changes in pH of SBF Post Incubation with BaBG. The alteration in the pH of SBF after immersion of BaBG at different time points during the *in vitro* pharmacokinetic study was measured for a period of 7 days using a calibrated pH meter.[20]

2.6. *In Vitro* Pharmacokinetic Study of BaBG. The leaching of dopants from the BG network with respect to time

https://doi.org/10.1021/acsomega.3c09250
ACS Omega 2024, 9, 7188−7205

was evaluated in SBF according to the technique suggested by the Technical Committee 4 (TC04) of the International Commission on Glass (ICG).[25] The *in vitro* pharmacokinetic study was performed by incubating the glass sample in SBF at a concentration of 1.5 mg/mL in an airtight polyethylene container to prevent any loss of media, hence avoiding any change in the ratio of glass/SBF. Throughout the experiment, the container was kept in an incubating orbital shaker maintained at 37 °C at 120 rpm. After 0.25, 0.5, 1, 2, 3, 6, 12, 24, 48, 72, 120, and 168 h, 5 mL of the solution was removed using a syringe. The solution was then passed through a 0.22 μm Millipore filter, and the concentrations of Si, Ca, and Ba were measured with ICP-MS and are expressed in ppm.

2.7. Animals. The animal experiment was carried out on adult healthy male albino Wistar rats (200 ± 20 g) that were procured from the Institutional Animal House, IMS- BHU, Varanasi, India. All of the experimental rats were acclimatized for 7 days to the laboratory environmental conditions in a controlled temperature of 25 ± 1 °C and a 45−55% relative humidity. All throughout the experimental protocol, the experimental animals were kept in a 12:12 h light/dark cycle with an *ad libitum* food (Paramount Laboratory Animal feed, Lanka, India) and water supply. During the experimental design, the National Institute of Health Guidelines (publication number 85−23, revised 2013) on animal care experimentation was followed to abridge the number of animals used. The entire experiment was accredited by the Central Animal Ethical Committee of the Indian Institute of Technology (Banaras Hindu University), Varanasi, India (ref no. IIT(BHU)/IAEC/2022/039).

2.8. Experimental Design for Single-Dose Oral *In Vivo* Pharmacokinetic Study. The *in vivo* oral pharmacokinetic study of BaBG was performed in Wistar rats that were divided into four groups: naive control, BaBG (1 mg/kg b.w.), BaBG (5 mg/kg b.w.), and BaBG (10 mg/kg b.w.) (Figure 1) using the randomization technique. Each group in the study had seven rats. BaBG was suspended in 0.5% CMC and administered orally to the overnight fasted experimental rats. Subsequently, blood was collected at 1, 24, 48, 72, 120, and 168 h post administration of BaBG from the lateral tail-vein of mildly anesthetized rats (anesthetized using diethyl ether) in heparinized centrifuge tubes. Plasma was collected immediately by centrifuging the blood samples at 4000*g* (Remi Centrifuge, model number C-24BL, India) for 10 min at 4 °C.[26] The supernatant was decanted and stored at −80 °C until further analysis.

2.9. Pharmacokinetic Analysis. Pharmacokinetic parameters like maximum plasma concentration (C_{max}) and the total time required to reach C_{max} (*i.e.*, T_{max}) of BaBG were obtained from the plasma concentration−time curve (AUC) of BaBG. Similarly, the mean residence time (MRT), half-life ($t_{1/2}$), volume of distribution (V_z), and clearance (CL) of BaBG were calculated *via* noncompartmental analysis using the PK Solver software, an "add-on" for Microsoft Excel.[27] All of the pharmacokinetic parameters are expressed as mean ± SD.

2.10. Analysis of Ca, Si, and Ba in Urine and Feces. To estimate the excretion of Ca, Si, and Ba into urine and feces, the experimental animals during the oral pharmacokinetic study were housed in metabolic cages for sample collection. The urine and fecal samples from each group were collected at the same time points of the pharmacokinetic experimental protocol for evaluating the urinary and fecal excretion of elements (*i.e.*, 0−1, 1−24, 24−48, 48−72, 72−120, 120−168, and 168−192 h). They were weighed immediately, chemically digested, and analyzed by ICP-MS for the presence of Ca, Si, and Ba.

2.11. Experimental Design for *In Vivo* Biodistribution Study after Single- Dose Oral Administration of BaBG. To estimate the distribution of dopants released from BaBG in various organs, the rats were randomly divided into four groups: naive control, BaBG (1 mg/kg bw), BaBG (5 mg/kg bw), and BaBG (10 mg/kg b.w.) (n = 6 rats/group). The same dose of BaBG that was used during the *in vivo* pharmacokinetic study was selected and administered orally in the rats (Figure 2). Post dosing, at distinct time points (days 1, 3, 5, and 7), the rats of each group were anesthetized using 3% v/v of isoflurane inhalation. Then, the animals were sacrificed by cervical dislocation, and vital organs like the brain, heart, lungs, liver,

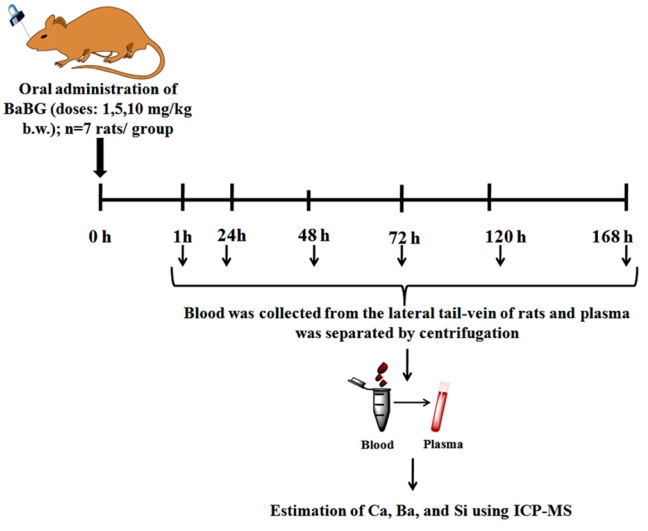

Figure 1. Schematic representation of the experimental protocol of the *in vivo* single-dose oral pharmacokinetics study of BaBG. The image was drawn using ChemDraw 15.0.

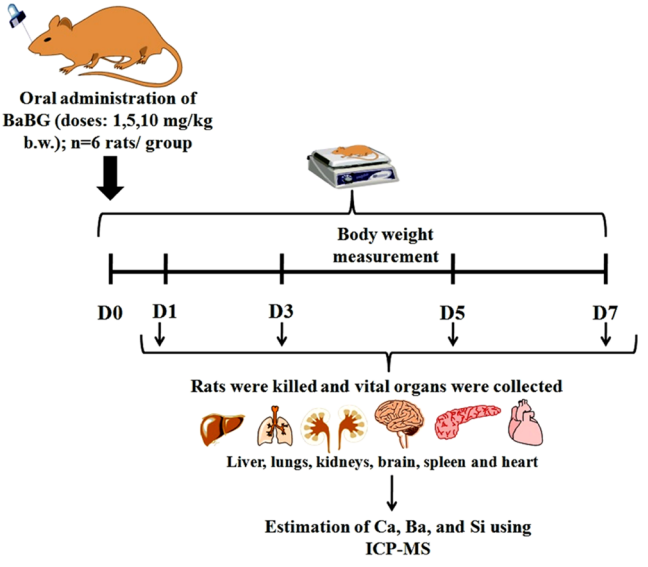

Figure 2. Schematic representation of the experimental protocol of the *in vivo* biodistribution study after single-dose oral administration of BaBG. The image has been drawn using ChemDraw 15.0.

https://doi.org/10.1021/acsomega.3c09250
ACS Omega 2024, 9, 7188−7205

kidneys, and spleen were dissected. The organs were weighed and processed for digestion and ICP-MS. The SEM analysis was performed to access the formation of HA as well as the surface morphological changes of all of the organs collected from the rats of the highest dose group (*i.e.*, 10 mg/kg b.w.) at day 7 post dosing.

2.12. Scanning Electron Microscopy (SEM) of Vital Organs. The vital organs like the brain, heart, lungs, kidneys, liver, and spleen collected were fixed in 2.5% glutaraldehyde solution overnight at 4 °C followed by washing in PBS thrice. Then, the tissue samples were dehydrated in a graded series of acetone and dried thoroughly. Subsequently, the dried tissue samples were gold−palladium-coated (EMITECH SC 7620) and viewed under the scanning electron microscope (Zeiss EVO LS 10, Carl Zeiss Ltd., Germany) at 10 kV.

2.13. Digestion of the Biological Samples for ICP-MS. Tissue samples of around 300 mg of the vital organs (brain, heart, lungs, kidneys, liver, and spleen) were predigested in an acidic condition by incubating the biological samples in a 3 mL mixture of nitric acid and perchloric acid (9:1) for 24 h. Then, the above mixture was heated at 80 °C for 10 h and again at 140 °C for 30 min. Later on, 2−3 mL of a mixture of nitric acid and perchloric acid was added to the reacting vessel to digest the residue and was further heated at 145 °C until the samples were evaporated to dryness. Finally, 2% v/v of nitric acid solution was added to dissolve the residues and filtered with Whatman filter paper (grade 1, pore size of 11 μm). The filtrate obtained was then diluted to make up the volume up to 5 mL. Similarly, the plasma (300 μL), urine (300 μL), and fecal samples (300 mg) were collected and digested as per the protocol followed for the tissue samples.[28]

2.14. Inductively Coupled Plasma Mass Spectroscopy (ICP-MS). The concentration of Ca, Si, and Ba present in the digested solutions was performed using ICP-MS, which is a single quadrupole type [iCAP-RQ (Thermofisher Scientific)]. The external calibration technique was followed for the quantitative analysis of the samples. The calibration curves for all of the analytes were built on 8 different concentrations (0.5−100 ppb) from the limit of detection (LOD) of the corresponding element, with the intention that concentrations of all analytes in the samples were within the linear range of the calibration curve. The calibration standards were analyzed at regular intervals during analysis to monitor the instrument drift. Also, ultrapure deionized water blanks were frequently used in the study alongside the samples to check for any loss or cross-contamination. All of the measurements were carried out using the full quantitative analysis mode.

2.15. Body Weight and Organ Coefficient. During the biodistribution study, the body weight of the animals in each group was weighed before and after BaBG administration. Similarly, at the end of biodistribution experiment for each time point, the organ (brain, heart, lungs, liver, kidneys, and spleen) weight was recorded and the organ coefficient for every time point was calculated using the following formulas

$$\text{organ coefficient} = \left[\frac{\text{weight of the organ (g)}}{\text{total body weight (g)}}\right] \times 100$$

2.16. Statistical Analysis. All of the data were analyzed statistically by GraphPad Prism ver. 8.0 (San Diego, CA, RRID: SCR_002798). The *in vivo* pharmacokinetic parameters for the released ions were assessed statistically by one-way ANOVA followed by Tukey's multiple comparison tests. The two-way ANOVA followed by the Bonferroni post hoc test was used to statistically analyze the plasma concentration profile, urinary and fecal excretion, body weight, organ coefficients, and biodistribution of Ca, Ba, and Si. We have considered $p < 0.05$ to be statistically significant in all of the analyses, and all of the values were presented as mean ± SD.

3. RESULTS AND DISCUSSION

3.1. Characterization of BaBG before and after Treatment with SBF Solution. The specific surface area and porosity of any compound are the important physico-chemical properties that determine the rate of dissolution and release kinetics of the glass matrix and thus the oral absorption when used therapeutically. Therefore, understanding these properties is crucial in drug development and in the present study; BET analysis was used to measure specific surface area and porosity. The N_2 adsorption−desorption isotherm for BaBG is represented in Figure S1, which was obtained at varying relative pressure and was in the shape of an H3 hysteresis loop as reported previously.[20] The isotherm resembles type IV, indicating sharp adsorption property with wider pore distributions.[29] Further, the presence of smaller hysteresis in the isotherm represents the capillary condensation phenomenon, which is typically observed in mesoporous compounds. Further, the average pore diameter, which was calculated using the BJH method, was found to be 36.63 nm. Therefore, it can be affirmed that BaBG is mesoporous in nature according to the IUPAC classification. Mesoporous biomaterials have been reported to have improved ionic dissolution and hence better therapeutic efficacy.[30] Similarly, the BET-specific surface area of BaBG was 2.04 m^2/g and the total pore volume was 0.0194 cm^3/g. Further, the mean particle size of BaBG was 431 ± 61.04 nm (Figure S3). Hence, it can be ascertained that BaBG has higher surface area due to smaller particle size, which enables them to have better contact with the body fluids with increased wettability, a desirable feature for drug/ion release kinetics with enhanced oral bioavailability during therapeutic applications.[30,31] Besides, the high mesoporosity and surface-area-to-volume ratio of the sol−gel-derived BaBG will allow more entrapment and sustainable release of the therapeutic substances, including metal ions, drugs, phytopharmaceuticals, and macromolecules (*e.g.*, proteins and DNA).[32]

Normally, inorganic biomaterials have the tendency to leach network modifiers in the physiological milieu along with hydroxyapatite (HA) formation, which helps in the adhesion of various proteins and growth factors, essential for tissue restoration.[33] Therefore, in the present study, the phase analysis was performed by XRD before and after treatment with SBF for 7 days and is depicted in Figure S2. The broad hump observed at 2θ ranging from 20° and 30° before the SBF treatment is an indication of the glassy characteristics of inorganic BGs, hence confirming its amorphous nature. However, incubation of BaBG in SBF for 7 days exhibited the appearance of newer crystalline peaks, therefore affirming its ability to form HA (calcium phosphate hydroxide), which correlates with the SEM result (Figure 4). The sharp crystalline peaks correspond to the hexagonal HA and are formed at 2θ = 22.93, 31.96, 35.46, 39.05, 42.61, 46.74, and 48.41° of *hkl* planes (111), (211), (301), (130), (302), (222), and (230), respectively (JCPDS # 74-0566).[20] A similar trend was observed in our previous study where increasing the duration of SBF treatment increased the intensity of the peak

https://doi.org/10.1021/acsomega.3c09250
ACS Omega 2024, 9, 7188−7205

corresponding to HA.[34] In addition, there is a prominent sharp peak corresponding to calcite ($CaCO_3$) formed at $2\theta = 29.22°$ of the *hkl* plane 104 and is rhombohedral in structure (JCPDS # 83-0578).[35] Several studies revealed that the formation of calcite is dependent on the size and porosity of BG[36] and the porous nature promotes the rapid leaching of Ca^{2+} ions into the SBF and hence precipitation of calcite. Calcite is reported to be biocompatible as evident by the oral acute and subacute toxicity studies performed on Wistar rats according to the OECD guidelines.[22]

Furthermore, the FTIR transmittance spectra of BaBG before and after SBF treatment are depicted in Figure 3 and

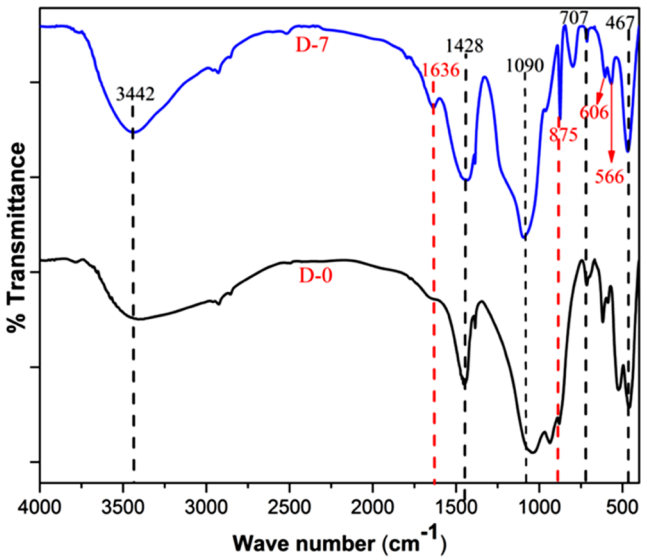

Figure 3. FTIR transmittance spectra of BaBG before and after soaking in the SBF solution for 7 days. The newer bands formed after the SBF treatment is marked in a red dashed line.

bands centered at around 467 and 707 cm^{-1} was observed. These bands correspond to the Si−O−Si symmetric bending and stretching, respectively, of the NBO (nonbinding oxygen) atoms between SiO_4 tetrahedral networks of BaBG formed due to the polymerization of the silanol group.[37] Further, another peak that may be due to the Si−O−Si asymmetrical stretching was observed at 1090 cm^{-1}. Similarly, at 1428 cm^{-1}, another band that was reported to be associated with the stretching mode of the C−O vibration of the carbonate group was observed in the FTIR spectra, mainly formed due to the interaction of BaBG with the atmospheric CO_2.[38] A very broad peak at 3442 cm^{-1} was also recorded that can be attributed to the OH group on the surface of the bioactive glass. However, after the SBF treatment for 7 days, newer divided vibration bands were visible at 566 and 606 cm^{-1}. These bands correspond to the P−O bending mode of vibrations[20] and therefore confirm the formation of a newer crystalline phase (calcium phosphate) as observed in SEM and XRD (Figures 4 and S2). Moreover, the band due to the P−O symmetrical stretching mode of vibration was centered at around 875 cm^{-1}. Thus, it can be concluded that the leaching of calcium from the BaBG matrix formed calcium phosphate hydroxide crystals (HA) after the SBF treatment. Additionally, at 1636 cm^{-1}, a newer band was observed that may be due to atmospheric CO_2 or precipitation of calcite as observed in XRD (Figure S2). Therefore, the *in vitro* bioactivity of BaBG can be concluded from the FTIR spectra following the incubation of BaBG with SBF. Moreover, the surface of SBF-treated BaBG was covered with irregularly grown crystals of HA of varying shape and size (Figure 4i(B)), thus correlating the results of XRD and FTIR. Likewise, in the EDX analysis, there was a decrease in Si from the glass surface with an increase in Ca and P concentrations (Figure 4ii(B)), showing dissolution of the silica framework of BaBG along with the *in situ* formation of crystalline HA.

3.2. The pH Behavior of BaBG in the SBF Solution.

The changes in pH of the SBF solution after soaking BaBG for a period of 7 days are shown in Figure 5. It has been observed that the pH of SBF solution was increased gradually and it attained maxima on day 3 (*i.e.*, 72 h) followed by a steady fall. In the present study, the pH of the solution elevated to 9.92 from the initial pH of SBF, which was 7.4. Incubation of BaBG

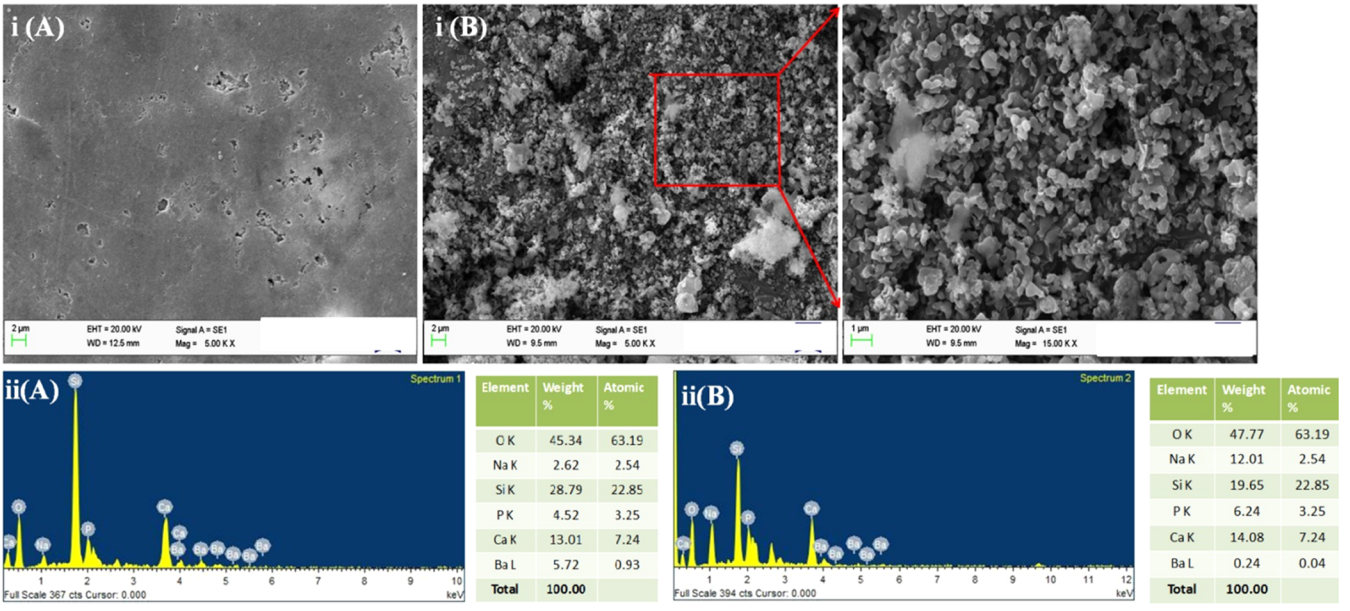

Element	Weight %	Atomic %
O K	45.34	63.19
Na K	2.62	2.54
Si K	28.79	22.85
P K	4.52	3.25
Ca K	13.01	7.24
Ba L	5.72	0.93
Total	100.00	

Element	Weight %	Atomic %
O K	47.77	63.19
Na K	12.01	2.54
Si K	19.65	22.85
P K	6.24	3.25
Ca K	14.08	7.24
Ba L	0.24	0.04
Total	100.00	

Figure 4. SEM micrographs and EDX analysis of BaBG before (iA) and (iiA) and after (iB) and (iiB) 7 days of treatment with SBF.

https://doi.org/10.1021/acsomega.3c09250
ACS Omega 2024, 9, 7188−7205

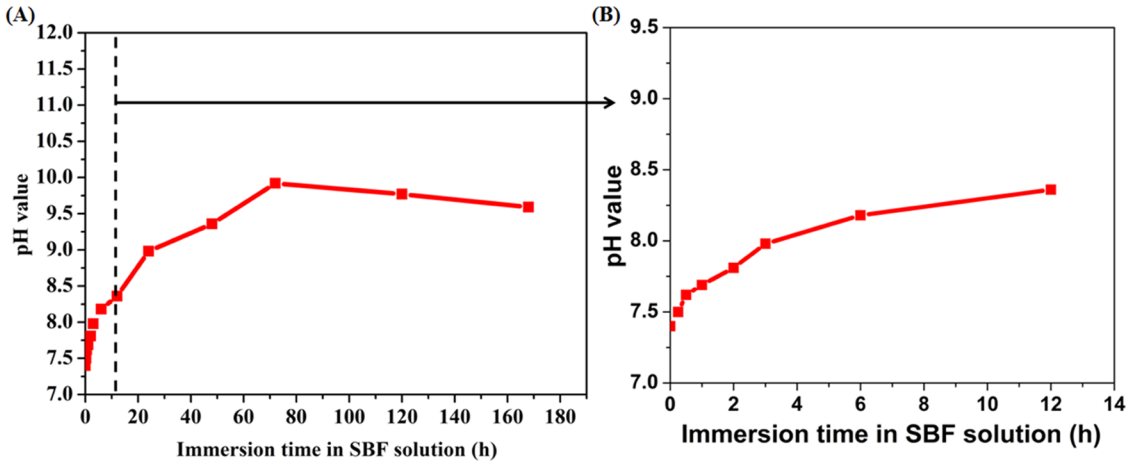

Figure 5. Changes in the pH of SBF solution after soaking BaBG for 7 days (A) and 12 h (B) during the *in vitro* pharmacokinetic study. The arrow depicts the zoomed version of panel A between 0 and 12 h.

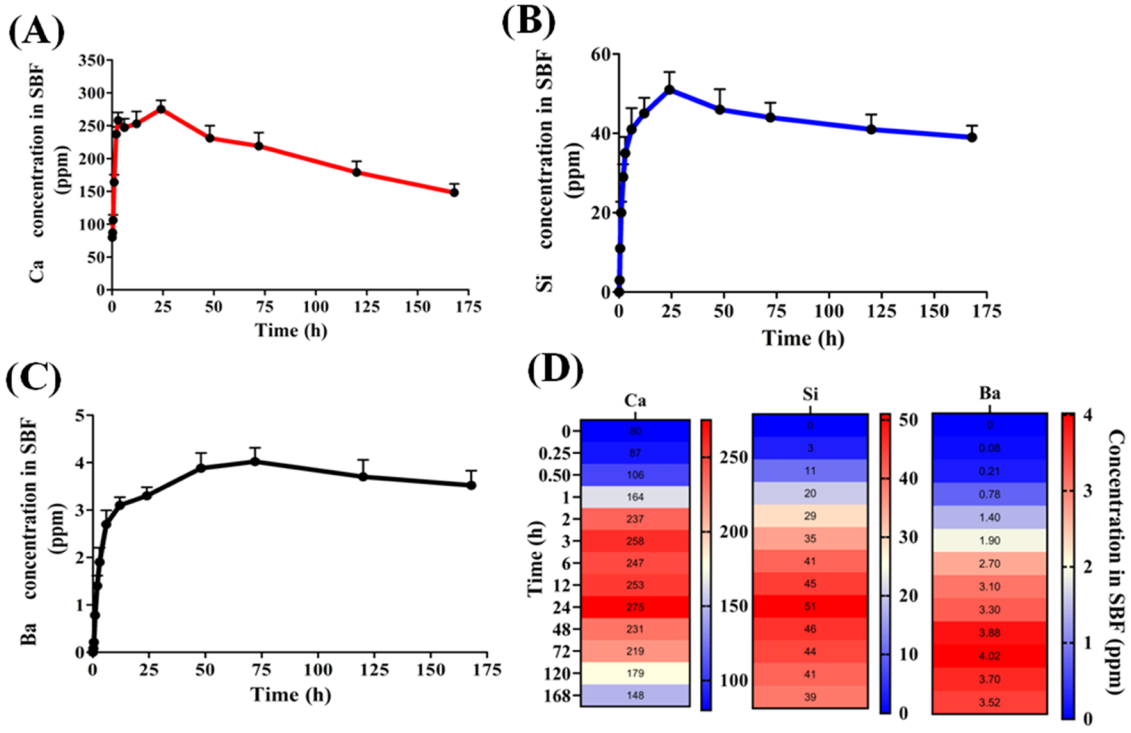

Figure 6. Release pattern of Ca (A), Si (B), and Ba (C) in SBF solution at pH 7.4 from BaBG at various time intervals for 7 days using ICP-MS and their representation by heatmap (D).

in SBF caused network dissolution of the Si−O−Si bonds and formation of silanol (Si−OH) groups that increased the pH of the surrounding solution. This causes leaching of cations entrapped in the glass matrix like Ca^{2+}, Ba^{2+}, and Na^{+} ions in exchange with H^{+} and H_3O^{+} from the surrounding media.[16,20] Thereafter, the pH of SBF was observed to decrease on reaching the ceiling at day 3 due to the precipitation of leached Ca^{2+} ions onto the negatively charged silica-rich surface. This leads to the entrapment of PO_4^{3-} ions from the SBF solution to form an amorphous calcium phosphate layer.[39] The crystalline apatite layer constitutes a physical barrier on the BaBG surface, hindering further ionic exchange, which limits the further change in the pH of SBF. In the event of extrapolation to *in vivo* conditions, the elevation of pH may influence the biokinetics of BaBG.

3.3. Temporal *In Vitro* Release of Ca, Si, and Ba from BaBG in SBF Solution. Normally, when BGs react with any physiological fluid like SBF, structural and chemical changes occur, and it progresses as a function of time, leading to the accumulation of dissolution products. This series of events ultimately causes an alteration in the ionic composition and thus the pH of the reacting fluid. The release of Ca, Si, and Ba from BaBG post-immersion in SBF solution with respect to time is shown in Figure 6. After the incubation of BaBG in SBF, the Ca level increased significantly (*i.e.*, 106 ppm) compared to the initial concentration (*i.e.*, 80 ppm) within 30 min (Figure 6A). Further, at 1 h, the Ca concentration was 164 ppm and then it increased to 275 ppm at 24 h. According to the theory proposed by Hench et al.[16] on the biomineralization of BGs, the increase in the level of Ca is due to dissolution of

https://doi.org/10.1021/acsomega.3c09250
ACS Omega 2024, 9, 7188−7205

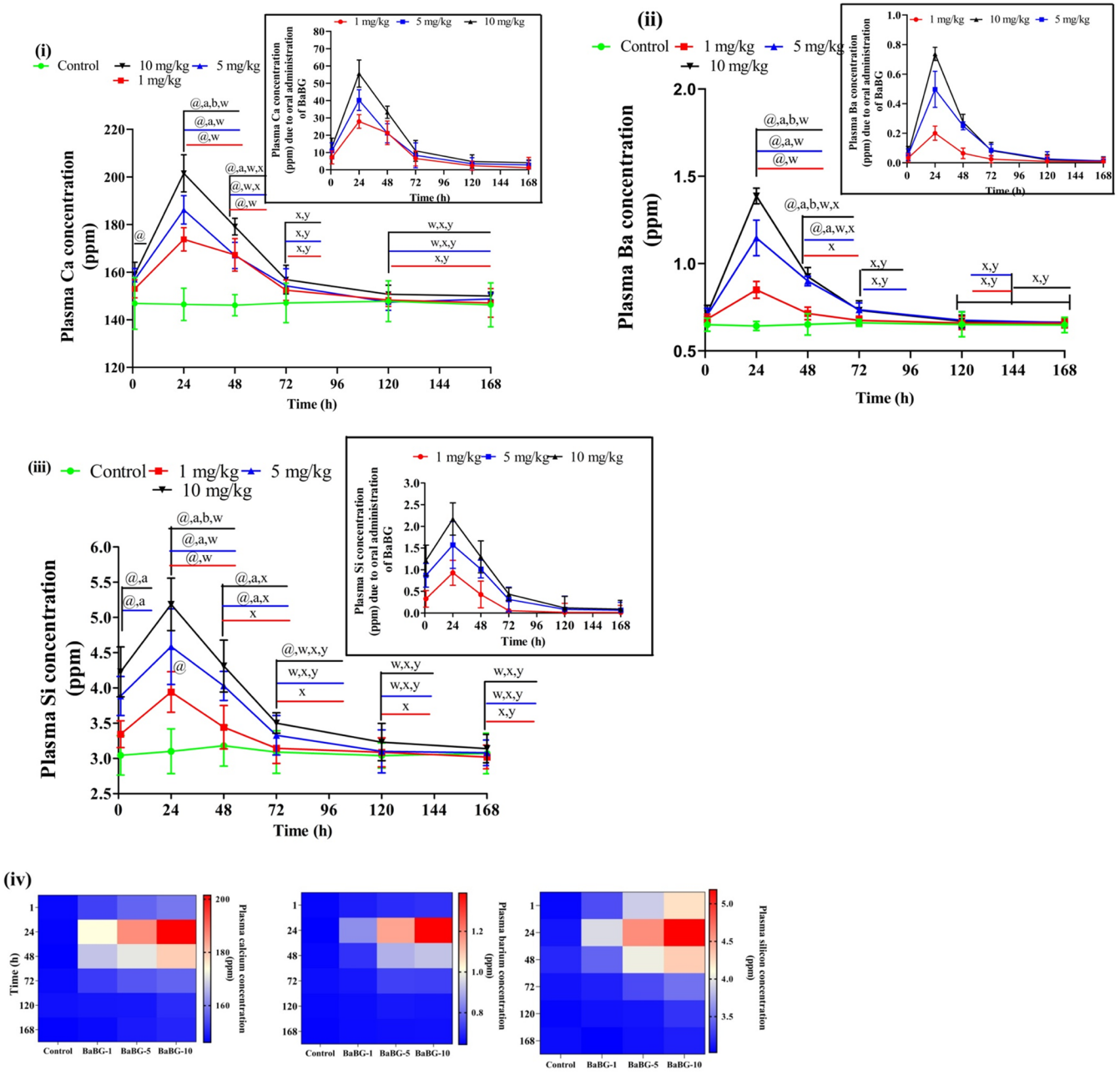

Figure 7. Plasma concentration profile of Ca (i), Ba (ii), and Si (iii) released from BaBG administered orally with the heatmap representation of the plasma concentration of Ca, Ba, and Si (iv). All values are in mean ± SD (n = 7 rats/group). $^{@}p < 0.05$, $^{a}p < 0.05$, and $^{b}p < 0.05$ compared to control, doses 1 and 5 mg/kg of BaBG, respectively. $^{w}p < 0.05$, $^{x}p < 0.05$, and $^{y}p < 0.05$ compared to 1, 24, and 48 h, respectively (two-way ANOVA followed by Bonferroni post hoc test).

the silica framework that leads to rapid leaching of cationic alkali/alkaline earth elements present as oxide network modifiers in the glasses in exchange with H^+/H_3O^+ from the SBF solution. Subsequently, there is a sharp reduction in the Ca concentration from day 3 (72 h) onward, and the Ca level was estimated to be around 148 ppm on day 7 (168 h). This indicates the migration of leached calcium along with phosphate from SBF to a silanol-rich layer on the surface of BaBG. The migration of the elements is considered essential as it leads to nucleation to form calcium phosphate, the precursor of amorphous HA.

Similarly, the concentration of Si was increased and then gradually decreased, as shown in Figure 6B and reaching maxima at 24 h (*i.e.*, 51 ppm). The composition of SBF as proposed by Kokubo et al.[23] has no Si present in it; thus, the appearance of Si after immersion of BaBG would have come from the degradation of silica networks in BaBG in a time-dependent manner. However, after 24 h, the level of Si fell steadily until the last day of immersion (*i.e.*, day 7). This reduction in Si may be due to the fact that the leached Si in SBF solution condenses and repolymerizes to form the negatively charged silanol.[16] Additionally, the amorphous HA layer also starts to deposit on the surface of BaBG, acting as a barrier between the BG surface and SBF, hence preventing further degradation of the silica network. Likewise, the leaching profile of the network modifiers in BaBG, *i.e.*, Ba, is represented in its release curve, *i.e.*, Figure 6C, and it exhibited a slow increase within the first few hours, reaching the maximum

https://doi.org/10.1021/acsomega.3c09250
ACS Omega 2024, 9, 7188−7205

concentration followed by a reduction in their concentration. The initial phase of release can be attributed to the surface Ba or the isolated Ba species trapped in the vitreous matrix and therefore it does not require extra energy to break the bonds and leach immediately. Further, the later phase of ionic release is due to the incorporated dopants inside the glass matrix. Ba^{2+} has larger ionic radius (135 pm) compared to Ca^{2+} (ionic radius is 100 pm) that causes an expanded glass network and decreased oxygen density.[20] Thus, there is more leaching of the cationic ions from doped BGs than from the parent 45S5. Previously, it has also been reported that the incorporation of barium in BaBG has increased the pH of the SBF solution compared to the undoped 45S5, thus confirming the dissolution of the silica matrix and release of Ca, Si, and Ba.[20]

3.4. *In Vivo* Oral Pharmacokinetic Study. *3.4.1. The Plasma Concentration of Ca, Ba, and Si Released from BaBG in Rats during the In Vivo Pharmacokinetic Study.* The plasma concentration of the leached Ca, Ba, and Si from BaBG after the oral administration at doses 1, 5, and 10 mg/kg was determined and is represented in Figure 7i, ii, and iii, respectively. The leaching profile of network modifiers is an essential parameter that needs to be evaluated before using inorganic biomaterials therapeutically as they tend to leach dopants that produce several biological effects at the physiological level. However, an increase in their level in the body beyond the physiological level can produce various physicochemical, pharmacokinetic, and pharmacodynamic interactions. For instance, antibiotics like tetracycline have been reported to form insoluble metal ion chelation with Ca that reduces its absorption, which can affect the bioavailability.[40] Further, the presence of excessive Ca may produce major drug interactions with calcium channel blockers and antiepileptic drugs.[41] Therefore, the *in vivo* release kinetics of the leached dopants from the matrix of BaBG was evaluated. In the present study, the plasma concentration−time curve of Ca and Ba exhibited a dose-dependent increase in their concentration in the plasma from the first hours, reaching maxima at 24 h, and then slowly decreased to the basal level by the end of the experimental protocol (shown in Figure 7i,ii). The plasma level of Ba increased maximum to 1.38 ppm at a dose of 10 mg/kg b.w. BaBG (reference level of Ba in the serum of control rats is reported to be around 0.6 ppm[42]). Similarly, the calcium level in the plasma of BaBG-treated rats was increased to 55.6 ppm at the highest dose of 10 mg/kg b.w. Statistical analysis by two-way ANOVA revealed significant changes in calcium and barium concentration in the plasma among the groups ($[F_{(3,144)} = 78.84; p < 0.05]$) and ($[F_{(3,144)} = 164.8; p < 0.05]$), respectively, time ($[F_{(5,144)} = 103.8; p < 0.05]$) and ($[F_{(5,144)} = 244.1; p < 0.05]$), respectively, and their interaction ($[F_{(15,144)} = 15.49; p < 0.05]$) and ($[F_{(15,144)} = 53.57; p < 0.05]$), respectively. The Bonferroni post hoc analysis revealed a significant increase in the level of both Ca and Ba at 24 and 48 h at all of the doses tested compared to the control rats. The above-observed result suggests that the cations doped in the BG framework were leached in exchange with the H^+ from the acidic gastric fluid in the stomach.[6] These released ions are considered to activate the cascade of proteins required for cellular activity over a period of time, which may be one of the reasons for the regenerative properties of BaBG in the *in vitro* model of neurotrauma.[20] Further, every element in our body has a physiological and pharmacological limit, and an uncontrolled and unchecked release of therapeutic dopants from BGs may lead to adverse effects. In this case, the increase in the level of Ba is within the safety limits and is also considered nontoxic as per the acute and subacute oral toxicity studies performed in rats.[22]

The network modifiers, *i.e.*, Ca and Ba, after their uphill increment until 24 h showed a gradual dip in their concentration in the plasma. The gradual decrease in calcium concentration in plasma after 24 h may be due to its accumulation over the silanol-rich layer forming an amorphous HA layer (as observed in XRD and FTIR during *in vitro* study). Additionally, since Ca is an endogenous element in the body, therefore an increase in its level is re-established naturally to the basal level through various physiological pathways. There are many calcium homeostasis-maintaining mechanisms that include its influx and efflux by the activation of various calcium transporter/channels, hormonal regulation through calcitonin, parathyroid hormone, and vitamin D3 and also by deposition in various organs and bones.[43] Similarly, the decrease in the level of Ba after 24 h may be because it is rapidly excreted out of the body mainly through the fecal matter, as observed during the excretion studies (Table 6). Moreover, there was a dose-dependent increase in the clearance (CL) of Ba from the plasma, and at dose 10 mg/kg, CL increased by around 3-fold compared to 1 mg/kg (Table 2). Ba accumulated mainly in the metabolizing and excretory organs, such as the liver and kidneys (Table 7). Ba has also been reported to get deposited mostly in the hard osseous tissues like the skeleton and teeth and also in fats,[44,45] which may have caused the decrease in the Ba plasma level after the observed C_{max} at 24 h (Table 2).

Similarly, after the oral administration of BaBG, there was a statistically significant increase in the level of Si in plasma at all doses compared with that of the control rats followed by a gradual decrease (as shown in Figure 7iii). The reference level of the reported Si level in control rats is 3 ppm.[46] The initial phase of the increased Si in the plasma of treated rats may be due to dissolution of the silicate networks of BaBG in the presence of physiological fluid.[16] Then, the leached Si is absorbed into the systemic circulation through the gastrointestinal epithelium. However, by the end of day 3, the elevated level of Si was found to be statistically insignificant, and at the end of day 7, it was similar to the basal level of Si present in the plasma of control rodents. This reduction in the level of Si may be due to the biodistribution of Si to various tissue compartments. Meanwhile, after the oral administration of BaBG, Si was remarkably higher in the spleen and liver, which may be due to the uptake by the reticuloendothelial system (RES) and Kupffer cells, respectively (as represented in Table 7), as similarly reported by Lee et al.[47]

3.4.2. In Vivo Oral Pharmacokinetic Profile of Ca, Ba, and Si Released from BaBG. The addition of network modifiers like CaO and BaO into the silica network of BGs tends to change the framework of BaBG, which may alter the dissolution kinetics and hence the pharmacokinetic parameters. Therefore, the pharmacokinetic parameters of the released therapeutic ions (Ca, Ba, and Si) from BaBG after its oral administration were estimated and are reported in Tables 1−3, respectively. The maximum concentration of Ca observed in the plasma (C_{max}) after the oral administration at doses 1, 5, and 10 mg/kg was 27.93 ± 3.02, 40.28 ± 5.19, and 55.62 ± 4.48 ppm, respectively, and statistical analysis by one-way ANOVA followed by Tukey's post hoc test revealed significant differences between them. However, the time taken to reach C_{max} (*i.e.*, T_{max}) was the same for all of the doses and was

https://doi.org/10.1021/acsomega.3c09250
ACS Omega 2024, 9, 7188−7205

Table 1. Pharmacokinetic Parameters for Ca Released after Single-Dose Oral Administration of BaBG[a]

pharmacokinetic parameters	1 mg/kg BaBG	5 mg/kg BaBG	10 mg/kg BaBG
half-life ($t_{1/2}$) (h)	39.27 ± 3.72	37.08 ± 2.99	36.85 ± 3.08
T_{max}(h)	24	24	24
C_{max}(ppm)	27.93 ± 3.02	40.28 ± 5.19[b]	55.62 ± 4.48[b,c]
AUC_{0-t} (ppm·h)	1636.01 ± 32.98	2127.17 ± 27.38[b]	2989.02 ± 40.96[b,c]
V_z (mg/kg)/(ppm)	0.0332 ± 0.002	0.1171 ± 0.003[b]	0.1657 ± 0.021[b,c]
CL (mg/kg)/(ppm)/h	0.00058 ± 0.000071	0.00219 ± 0.00025[b]	0.00311 ± 0.00039[b,c]
MRT (h)	53.72 ± 5.34	59.12 ± 4.90	59.59 ± 4.16

[a]All data are expressed as mean ± SD (n = 7 male rats/group). [b]$p < 0.05$ and [c]$p < 0.05$ compared to 1 and 5 mg/kg b.w., respectively (one-way ANOVA followed by Tukey's multiple comparison post hoc tests).

Table 2. Pharmacokinetic Parameters for Ba Released after Single-Dose Oral Administration of BaBG[a]

pharmacokinetic parameters	1 mg/kg BaBG	5 mg/kg BaBG	10 mg/kg BaBG
half-life ($t_{1/2}$) (h)	31.62 ± 2.88	26.47 ± 2.05[b]	24.72 ± 2.71[b]
T_{max}(h)	24	24	24
C_{max}(ppm)	0.22 ± 0.0189	0.49 ± 0.0488[b]	0.73 ± 0.064[b,c]
AUC_{0-t} (ppm·h)	8.804 ± 0.65	23.67 ± 1.93[b]	28.97 ± 2.52[b,c]
V_z (mg/kg)/(ppm)	4.961 ± 0.37	7.904 ± 0.84[b]	12.101 ± 0.99[b,c]
CL (mg/kg)/(ppm)/h	0.109 ± 0.0078	0.207 ± 0.0154[b]	0.339 ± 0.0316[b,c]
MRT (h)	48.26 ± 3.91	46.79 ± 4.05	41.51 ± 3.98[b]

[a]All data are expressed as mean ± SD (n = 7 male rats/group). [b]$p < 0.05$ and [c]$p < 0.05$ compared to 1 and 5 mg/kg b.w., respectively (one-way ANOVA followed by Tukey's multiple comparison post hoc tests).

Table 3. Pharmacokinetic Parameters for Si Released after Single-Dose Oral Administration of BaBG[a]

pharmacokinetic parameters	1 mg/kg BaBG	5 mg/kg BaBG	10 mg/kg BaBG
half-life ($t_{1/2}$) (h)	22.31 ± 2.51	29.24 ± 1.96[b]	29.95 ± 3.04[b]
T_{max}(h)	24	24	24
C_{max}(ppm)	0.93 ± 0.073	1.57 ± 0.184[b]	2.18 ± 0.206[b,c]
AUC_{0-t} (ppm·h)	39.24 ± 4.26	88.73 ± 7.21[b]	120.32 ± 9.13[b,c]
V_z (mg/kg)/(ppm)	0.812 ± 0.071	2.305 ± 0.181[b]	3.432 ± 0.244[b,c]
CL (mg/kg)/(ppm)/h	0.0252 ± 0.0019	0.054 ± 0.0043[b]	0.081 ± 0.0075[b,c]
MRT (h)	35.33 ± 3.04	46.13 ± 4.13[b]	47.17 ± 3.86[b]

[a]All data are expressed as mean ± SD (n = 7 male rats/group). [b]$p < 0.05$ and [c]$p < 0.05$ compared to 1 and 5 mg/kg b.w., respectively (one-way ANOVA followed by Tukey's multiple comparison post hoc tests).

observed at 24 h. Moreover, the time taken for the concentration of Ca in plasma to reduce by 50% (*i.e.*, $t_{1/2}$) was found to be 39.27 ± 3.72, 37.08 ± 2.99, and 36.85 ± 3.08 h for 1, 5, and 10 mg/kg, respectively, and was statistically insignificant ($p > 0.05$). We also observed that the volume of distribution (V_z) and mean residence time (MRT) for Ca were increased in a dose-dependent manner (as shown in Table 1). Since $t_{1/2}$ is a composite pharmacokinetic parameter, which is determined by V_z, hence, it can be ascertained that Ca in the blood circulation is biodistributed and is more concentrated in tissue compartments than in the vascular compartment of the body after its release from BaBG, which correlated with the biodistribution study results (Table 7). Further, with an increase in dose, Ca leached from BaBG exhibited longer MRT. This may be due to the reason that around 98% of filtered Ca gets reabsorbed by the renal tubules of kidneys[48] by passive diffusion or solvent drag under normal physiological conditions. Additionally, the increased Ca is also removed from the blood circulation by binding to serum albumin noncovalently,[48] hence longer MRT with the increase in the dose of BaBG.

Similarly, after the oral administration of BaBG, Ba ions are leached from the BG framework and enter the systemic circulation by absorption through the biological membrane. The course of movement of the leached dopants throughout the body before their excretion is essential to elucidate the extent of therapeutic effects, as well as the toxic effects they might produce. Hence, the pharmacokinetic parameters of Ba released from BaBG were determined and are represented in Table 2. In the present study, after the leaching of Ba in the GIT, they are absorbed, which caused a significant increase in the C_{max} of Ba in a dose-dependent manner similar to Ca in plasma. The T_{max} was observed at 24 h for all of the doses. The C_{max} increased to more than double at dose 5 mg/kg b.w. (*i.e.*, 0.49 ± 0.0488 ppm) compared to 1 mg/kg (0.22 ± 0.0189 ppm). Similarly, at dose 10 mg/kg, C_{max} increased significantly to 1.38 ppm compared to both doses (1 and 5 mg/kg b.w.; $p < 0.05$). The increased C_{max} for Ba in plasma with dose sheds light on the fact that the leached barium was absorbed through the gastrointestinal epithelium and reached the blood circulation. However, contrary to Ca, the $t_{1/2}$ and MRT for Ba decreased in a dose-dependent manner, and the specific reason explaining this trend remains unclear. The biodistribution pattern of the divalent Ba after their absorption from the GIT may help to explain this unusual trend. From the above results, it can also be presumed that after reaching the highest plasma concentration at 24 h, the physiological hemostasis set-point for barium is broken. As a result, irrespective of increased C_{max} with an increase in dose, there is a decrease in $t_{1/2}$ and MRT for doses of 5 and 10 mg/kg

https://doi.org/10.1021/acsomega.3c09250
ACS Omega 2024, 9, 7188−7205

compared to the lowest dose (*i.e.*, 1 mg/kg b.w.). In general, the body tries to maintain homeostasis by distributing it to other body compartments or by excreting it. It has been observed that biologically nonessential elements like Ba have the tendency to get rapidly deposited mainly in less perfused mineralized organs like the skeleton systems.[42,49] Ba having larger ionic radii than Ca gets more readily adsorbed in the form of colloidal particles on the surface of bones that help in the calcification process. Additionally, Ba was rapidly excreted in the feces since the body has the tendency to reduce the load of nonessential elements from the body as evidenced by the increased clearance (as represented in Table 5) with increased dose, which was statistically significant ($p < 0.05$). Therefore, from the above-mentioned results, we can say that the increased level of Ba in blood circulation is normalized by physiological homeostatic pathways including biodistribution and excretion.

Further, in the case of Si, the C_{max} increased with dose and was found to be 0.93 ± 0.073, 1.57 ± 0.184, and 2.18 ± 0.206 ppm for 1, 5, and 10 mg/kg b.w., respectively, and the T_{max} was observed at 24 h for all of the doses (as shown in Table 3). Furthermore, another important pharmacokinetic parameter is V_z, which was also found to be augmented by approximately 2.8- and 4.2-fold at doses 5 and 10 mg/kg compared to 1 mg/kg. Higher V_z indicates that the absorbed Si in the vascular compartment has a high tendency to escape the blood circulation and enter the extravascular compartments as observed during the biodistribution study (Table 7). Similarly, the MRT of Si in the body for doses 5 and 10 mg/kg was significantly higher compared to 1 mg/kg ($p < 0.05$), which can be due to enhanced distribution in various tissues. Studies have reported that Si accumulation in various organs, mainly the liver and spleen, was observed for 3 days in rats.[47] As per previous study, there was no accumulated organ toxicity of BaBG in rats when administered orally at a dose of up to 1000 mg/kg b.w.[22]

3.5. Urinary and Fecal Excretion. The inorganic biomaterials are considered biologically safe and can be translated clinically only if they have a controlled rate of elimination and metabolism. Therefore, the excretion kinetics of Ca, Ba, and Si released from BaBG after the oral administration was evaluated and is represented in Tables 4−6, respectively. The clearance of any inorganic compound from the body follows two major eliminating routes, *i.e.*, hepatobiliary and fecal excretion and the urinary excretion; hence, we temporally measured the level of Ca, Ba, and Si in urine and feces. It was observed that the cumulative amount of Ca excreted in urine and feces increased with the dose of BaBG (Table 4). Statistical analysis by two-way ANOVA exhibited significant changes in the Ca level in the urine and feces among the groups ($[F(_{3,168}) = 271.5; p < 0.05]$ and $[F(_{3,168}) = 162.5; p < 0.05]$, respectively), time ($[F(_{6,168}) = 1434; p < 0.05]$ and $[F(_{6,168}) = 2031; p < 0.05]$, respectively), and their interaction ($[F(_{18,168}) = 7.664; p < 0.05]$ and $[F(_{18,168}) = 5.606; p < 0.05]$, respectively). The post hoc analysis revealed a significant increase in the level of Ca in the urine and feces from 24 h onward at doses 5 and 10 mg/kg compared to the control group. The above-observed results have been similar to the previous report where calcium is excreted mainly through urine and feces to maintain the body's homeostasis.[50] However, after the glomerular filtration of Ca by kidneys, 80% of the filtered Ca is reabsorbed *via* passive diffusion or solvent drag in the proximal tubule.[50] It is also noteworthy that in our study the

Table 4. Urinary and Fecal Excretion of Ca Postoral Administration of BaBG in Rats[a]

doses of BaBG (mg/kg b.w.)	0−1 h	1−24 h	24−48 h	48−72 h	72−120 h	120−168 h	168−192 h
			Cumulative Amount Excreted in Urine (ppm)				
control	20.48 ± 3.78	38.88 ± 3.26	56.10 ± 4.91	77.49 ± 5.15	105.54 ± 6.84	120.37 ± 9.79	139.39 ± 3.27
1	22.19 ± 2.15	50.26 ± 4.26	75.65 ± 8.35^{b}	98.76 ± 7.84^{b}	118.69 ± 4.12^{b}	138.90 ± 7.23^{b}	154.94 ± 9.91^{b}
5	25.44 ± 2.03	59.57 ± 7.07^{b}	89.78 ± 6.07^{b,c}	112.26 ± 10.52^{b,c}	129.70 ± 10.83^{b,c}	147.78 ± 3.68^{b,c}	167.39 ± 5.38^{b,c}
10	26.32 ± 4.11	66.34 ± 5.73^{b,c}	101.14 ± 8.72^{b,c,d}	127.47 ± 5.37^{b,c,d}	157.58 ± 13.42^{b,c,d}	167.61 ± 7.71^{b,c,d}	181.87 ± 6.22^{b,c,d}
			Cumulative Amount Excreted in Feces (ppm)				
control	35.82 ± 1.45	74.13 ± 8.82	114.14 ± 13.20	146.19 ± 8.81	181.76 ± 14.49	220.47 ± 15.35	254.70 ± 18.02
1	33.03 ± 3.89	79.05 ± 9.16	121.32 ± 10.26	152.41 ± 6.78	192.63 ± 5.24	235.07 ± 6.16	275.45 ± 12.52^{b}
5	40.16 ± 4.19	93.67 ± 7.90^{b}	144.71 ± 11.33^{b,c}	175.38 ± 10.04^{b,c}	201.72 ± 10.72^{b,c}	251.57 ± 10.73^{b,c}	292.84 ± 9.75^{b,c}
10	37.54 ± 5.28	102.71 ± 12.23^{b,c}	161.82 ± 4.04^{b,c,d}	192.27 ± 5.27^{b,c,d}	235.25 ± 8.06^{b,c,d}	279.73 ± 11.47^{b,c,d}	310.80 ± 17.79^{b,c,d}

[a]Data are expressed as mean ± SD ($n = 7$ male rats/group). $^{b}p < 0.05$, $^{c}p < 0.05$, and $^{d}p < 0.05$ compared to control, 1, and 5 mg/kg b.w., respectively (two-way ANOVA followed by Bonferroni post hoc test).

https://doi.org/10.1021/acsomega.3c09250
ACS Omega 2024, 9, 7188−7205

Table 5. Urinary and Fecal Excretion of Ba Postoral Administration of BaBG in Rats[a]

doses of BaBG (mg/kg b.w.)	0−1 h	1−24 h	24−48 h	48−72 h	72−120 h	120−168 h	168−192 h
			Cumulative Amount Excreted in Urine (ppm)				
control	0.41 ± 0.083	0.78 ± 0.052	1.08 ± 0.28	1.35 ± 0.34	1.70 ± 0.20	2.12 ± 0.36	2.43 ± 0.42
1	0.39 ± 0.051	0.79 ± 0.094	1.41 ± 0.35	1.89 ± 0.19[b]	2.15 ± 0.37[b]	2.42 ± 0.28	2.80 ± 0.3
5	0.43 ± 0.037	0.96 ± 0.046	1.45 ± 0.18	1.92 ± 0.22[b]	2.21 ± 0.41[b]	2.69 ± 0.23[b]	3.11 ± 0.28[b,c]
10	0.48 ± 0.066	1.12 ± 0.18	1.70 ± 0.28[b]	2.20 ± 0.39[b]	2.67 ± 0.18[b,c,d]	3.15 ± 0.41[b,c,d]	3.61 ± 0.42[b,c,d]
			Cumulative Amount Excreted in Feces (ppm)				
control	0.38 ± 0.016	0.68 ± 0.092	1.08 ± 0.15	1.48 ± 0.17	1.83 ± 0.37	2.24 ± 0.14	2.68 ± 0.28
1	0.40 ± 0.025	0.84 ± 0.056	1.42 ± 0.21	1.91 ± 0.27[b]	2.33 ± 0.18[b]	2.72 ± 0.35[b]	3.06 ± 0.31
5	0.42 ± 0.073	0.89 ± 0.12	1.61 ± 0.17[b]	2.03 ± 0.29[b]	2.61 ± 0.39[b]	3.03 ± 0.44[b]	3.49 ± 0.46[b,c]
10	0.37 ± 0.028	1.12 ± 0.19	1.98 ± 0.24[b,c,d]	2.71 ± 0.35[b,c,d]	3.08 ± 0.42[b,c,d]	3.85 ± 0.41[b,c,d]	4.25 ± 0.57[b,c,d]

[a]Data are expressed as mean ± SD (n = 7 male rats/group). [b]$p < 0.05$, [c]$p < 0.05$, and [d]$p < 0.05$ compared to control, 1, and 5 mg/kg b.w., respectively (two-way ANOVA followed by Bonferroni post hoc test).

Table 6. Urinary and Fecal Excretion of Si Postoral Administration of BaBG in Rats[a]

doses of BaBG (mg/kg b.w.)	0−1 h	1−24 h	24−48 h	48−72 h	72−120h	120−168 h	168−192 h
			Cumulative Amount Excreted in Urine (ppm)				
control	1.03 ± 0.12	2.11 ± 0.27	2.64 ± 0.34	3.17 ± 0.18	3.75 ± 0.27	4.14 ± 0.28	4.73 ± 0.32
1	1.65 ± 0.19	2.36 ± 0.16	3.09 ± 0.32	3.68 ± 0.29[b]	4.22 ± 0.21[b]	4.81 ± 0.41[b]	5.32 ± 0.28[b]
5	1.51 ± 0.11	2.62 ± 0.23[b]	3.19 ± 0.39[b]	3.89 ± 0.24[b]	4.38 ± 0.13[b]	5.08 ± 0.51[b]	5.75 ± 0.41[b]
10	1.72 ± 0.17[b]	2.83 ± 0.24[b,c]	3.67 ± 0.40[b,c,d]	4.17 ± 0.38[b,c]	4.82 ± 0.36[b,c]	5.69 ± 0.33[b,c,d]	6.37 ± 0.74[b,c,d]
			Cumulative Amount Excreted in Feces (ppm)				
control	0.72 ± 0.17	1.72 ± 0.27	2.72 ± 0.35	3.78 ± 0.31	4.76 ± 0.64	5.89 ± 0.66	6.62 ± 0.85
1	1.01 ± 0.23	2.89 ± 0.15[b]	4.15 ± 0.39[b]	5.21 ± 0.27[b]	6.13 ± 0.46[b]	7.09 ± 0.37[b]	7.74 ± 0.43[b]
5	0.94 ± 0.084	3.19 ± 0.28[b]	4.39 ± 0.45[b]	5.84 ± 0.53[b,c]	7.01 ± 0.32[b,c]	7.81 ± 0.40[b,c]	8.88 ± 0.74[b,c]
10	0.88 ± 0.26	3.66 ± 0.13[b,c]	5.27 ± 0.35[b,c,d]	7.62 ± 0.49[b,c,d]	8.85 ± 0.61[b,c,d]	9.39 ± 0.54[b,c,d]	10.03 ± 0.52[b,c,d]

[a]Data are expressed as mean ± SD (n = 7 male rats/group). [b]$p < 0.05$, [c]$p < 0.05$, and [d]$p < 0.05$ compared to control, 1 mg/kg, and 5 mg/kg b.w. dose of BaBG, respectively (two-way ANOVA followed by Bonferroni post hoc test).

cumulative excretion of Ca was more in feces than in urine. We speculate that BaBG tends to get adsorbed into the mucous layer of the stomach after oral administration (Figure 9). This protective layer (mucus) has the tendency to continuously renew itself and is removed from the site, travels to the lower GIT, and is excreted in feces. Therefore, Ca released into the lower GIT from the trapped BaBG in mucus has less opportunity to get absorbed, leading to an increased Ca level in feces.

Similarly, in the excretion kinetic study of Ba, there was an increase in the level of Ba in both urine and feces dose-dependently like Ca (shown in Table 5). Normally, Ba released from BaBG is absorbed into the blood through the biological membrane of GIT and then the body tries to restore homeostasis by distributing to the bones and excretion through urine and feces.[45,51] Likewise, in our study, we observed that the plasma level of Ba after the oral administration of BaBG followed a downhill fall after the observed T_{max} at 24 h (Figure 7ii). The fall in the level of Ba may be due to increased clearance dose-dependently (Table 2) as Ba is a nonessential element and the body tries to eliminate it to restore homeostasis. We also observed that the fecal excretion of Ba exceeded urinary excretion. In support of our observation, a study published indicated feces to be the primary route of excretion of Ba in rats that were exposed to barium chloride in their diet.[52] Similarly, in the biodistribution study, the Ba level was more in the liver compared to that in the kidneys (Table 7). The deposited Ba in liver is most likely to get secreted in bile and thereby excreted out in feces.

The elimination kinetics of Si leached from BaBG after the single-dose oral administration is represented in Table 6, and statistical analysis by two-way ANOVA followed by post hoc test exhibited significant elevation in the level of Si in urine and feces compared to the control rats. The detection of Si in urine implies that kidneys are one of the excreting organs, and even in the biodistribution study of BaBG, Si was detected more in the kidneys and liver compared to that in other organs (Table 7). Normally, Si that enters the systemic circulation after absorption through the intestinal mucosa follows the renal route of excretion without affecting the microstructure of kidneys.[22]

3.6. Changes in Body Weight and Organ Coefficient after Oral Administration of BaBG. In the temporal biodistribution study of BaBG at different doses, the body weight and the organ coefficient of the treated rats were measured, as they are the essential parameters to ascertain the normal physiological functioning of the internal organs. Therefore, the body weight of the rats treated with BaBG at doses 1, 5, and 10 mg/kg were measured and are represented in Figure S4i. Statistical analysis by two-way ANOVA showed no significant differences between the body weights of rats in every group ($p > 0.05$). Moreover, the organ coefficients of various vital organs like the brain, heart, lungs, liver, kidneys, and spleen were also statistically insignificant ($p > 0.05$) compared to the control group (Figure S4ii−vii). This confirms that the doses selected for the pharmacokinetic and biodistribution study were safer and these findings are in agreement with our previous report[22] where BaBG was found

https://doi.org/10.1021/acsomega.3c09250
ACS Omega 2024, 9, 7188−7205

Table 7. Tissue Concentration of Ca, Ba, and Si in the Brain, Heart, Lungs, Liver, Kidneys, and Spleen after Single-Dose Oral Administration of BaBG at Doses 1, 5, and 10 mg/kg b.w. at Days 1, 3, 5, and 7[a]

(i)

	concentration of Ca (ppm) in brain				concentration of Ba (ppm) in brain			
	D1	D3	D5	D7	D1	D3	D5	D7
control	9.61 ± 1.78	10.23 ± 0.93	10.17 ± 1.22	9.74 ± 0.90	0.0067 ± 0.0014	0.0062 ± 0.00084	0.0060 ± 0.0011	0.0068 ± 0.0007
BaBG-1	10.28 ± 0.85	11.89 ± 1.43	9.92 ± 0.75[f]	9.87 ± 1.07[f]	0.0063 ± 0.0013	0.0072 ± 0.0006	0.0068 ± 0.0017	0.0066 ± 0.0005
BaBG-5	10.94 ± 1.71	12.27 ± 1.02[b]	10.01 ± 1.46[f]	9.63 ± 1.21[f]	0.0067 ± 0.0007	0.0078 ± 0.0012[b]	0.0070 ± 0.0004	0.0065 ± 0.0007
BaBG-10	11.53 ± 2.03[b]	12.92 ± 0.96[b]	10.38 ± 0.37[f]	10.11 ± 0.89[f]	0.0069 ± 0.0011	0.0081 ± 0.0003[b]	0.0071 ± 0.0012	0.0062 ± 0.0016[f]

(ii)

	concentration of Ca (ppm) in lungs				concentration of Ba (ppm) in lungs			
	D1	D3	D5	D7	D1	D3	D5	D7
control	157.62 ± 14.12	160.02 ± 13.98	151.91 ± 10.12	159.21 ± 16.04	0.045 ± 0.0068	0.050 ± 0.0044	0.049 ± 0.0086	0.044 ± 0.0071
BaBG-1	163.07 ± 12.17	171.11 ± 7.77	160.48 ± 9.83	158.96 ± 7.51	0.056 ± 0.0061	0.063 ± 0.0059[b]	0.050 ± 0.0028[f]	0.047 ± 0.0067[f]
BaBG-5	170.50 ± 6.91	180.56 ± 9.09[b]	161.23 ± 17.15[f]	163.60 ± 10.89	0.061 ± 0.0078[b]	0.072 ± 0.0034[b]	0.058 ± 0.0060[f]	0.049 ± 0.0054[f]
BaBG-10	177.68 ± 15.98[b]	191.78 ± 10.13[b,c]	167.41 ± 8.03[f]	160.70 ± 13.68[f]	0.070 ± 0.0044[b,c]	0.083 ± 0.0061[b,c,e]	0.061 ± 0.0081[f]	0.053 ± 0.023[e,f]

(iii)

	concentration of Ca (ppm) in Heart				concentration of Ba (ppm) in Heart			
	D1	D3	D5	D7	D1	D3	D5	D7
control	81.03 ± 10.93	84.35 ± 7.01	89.16 ± 8.80	80.99 ± 11.27	0.014 ± 0.0034	0.014 ± 0.0047	0.012 ± 0.0024	0.015 ± 0.0061
BaBG-1	89.02 ± 6.59	96.19 ± 10.11	80.22 ± 4.48[f]	84.41 ± 5.87	0.019 ± 0.0026	0.021 ± 0.0016	0.015 ± 0.0010	0.013 ± 0.0057[f]
BaBG-5	94.48 ± 12.03	100.39 ± 9.87[b]	90.78 ± 7.42	86.29 ± 6.26[f]	0.023 ± 0.0067[b]	0.034 ± 0.0073[b,c,e]	0.019 ± 0.0035[f]	0.015 ± 0.0072[e,f]
BaBG-10	101.66 ± 8.13[b,c]	113.01 ± 13.17[b,c]	96.97 ± 10.39[b,f]	82.72 ± 9.94[e,f,g]	0.030 ± 0.0051[b,c]	0.041 ± 0.0039[b,c,e]	0.021 ± 0.0060[b,e,f]	0.017 ± 0.0028[e,f]

(iv)

	concentration of Ca (ppm) in liver				concentration of Ba (ppm) in liver			
	D1	D3	D5	D7	D1	D3	D5	D7
control	9.36 ± 1.21	9.19 ± 1.09	9.40 ± 0.72	9.03 ± 0.83	0.072 ± 0.0081	0.078 ± 0.0093	0.074 ± 0.0055	0.080 ± 0.0123
BaBG-1	10.73 ± 1.25	11.85 ± 0.82[b]	9.18 ± 1.04[f]	9.41 ± 1.82[f]	0.096 ± 0.0230	0.119 ± 0.0207[b]	0.102 ± 0.0148[b]	0.088 ± 0.0038
BaBG-5	12.43 ± 1.09[b,c]	13.71 ± 0.91[b,c,e]	10.42 ± 0.96[e,f]	9.82 ± 0.52[e,f]	0.120 ± 0.0141[b]	0.148 ± 0.0209[b,c]	0.117 ± 0.0091[b]	0.095 ± 0.0106
BaBG-10	15.86 ± 1.31[b,c,d]	16.90 ± 1.19[b,c]	11.14 ± 0.61[f]	9.25 ± 0.68[e,f]	0.132 ± 0.0357[b,c]	0.169 ± 0.0258[b,c]	0.121 ± 0.0179[b]	0.098 ± 0.0128[f]

(v)

	concentration of Ca (ppm) in kidneys				concentration of Ba (ppm) in kidneys			
	D1	D3	D5	D7	D1	D3	D5	D7
control	93.42 ± 7.89	92.12 ± 4.12	95.19 ± 8.04	97.89 ± 6.43	0.038 ± 0.0041	0.042 ± 0.0063	0.034 ± 0.0048	0.041 ± 0.0069
BaBG-1	98.78 ± 10.82	109.83 ± 2.13[b,e]	94.28 ± 9.15[f]	95.93 ± 8.45[f]	0.044 ± 0.0076	0.056 ± 0.0092[b,e]	0.043 ± 0.0070[f]	0.038 ± 0.002[f]
BaBG-5	106.13 ± 2.91[b]	118.01 ± 2.24[b,e]	102.59 ± 10.27[f]	93.50 ± 4.98[e,f]	0.051 ± 0.0047[b]	0.069 ± 0.0103[b,c,e]	0.050 ± 0.0031[b,f]	0.044 ± 0.0050[f]
BaBG-10	115.70 ± 6.04[b,c]	132.33 ± 4.08[b,c,d,e]	106.86 ± 5.99[b,c,e,f]	95.57 ± 7.34[e,f]	0.060 ± 0.0089[b,c]	0.081 ± 0.0116[b,c,d,e]	0.061 ± 0.0064[b,c,d,f]	0.045 ± 0.0028[e,f,g]

https://doi.org/10.1021/acsomega.3c09250
ACS Omega 2024, 9, 7188−7205

Table 7. continued

	(vi) concentration of Ca (ppm) in spleen				concentration of Ba (ppm) in spleen			
	D1	D3	D5	D7	D1	D3	D5	D7
control	26.18 ± 3.45	25.03 ± 1.89	23.44 ± 2.25	26.12 ± 3.01	0.051 ± 0.0078	0.048 ± 0.0051	0.045 ± 0.0041	0.050 ± 0.0029
BaBG-1	30.67 ± 4.09	37.12 ± 3.58[b,e]	27.84 ± 3.18[f]	25.78 ± 2.26[e,f]	0.070 ± 0.0036	0.091 ± 0.0061[b]	0.073 ± 0.0082[b]	0.058 ± 0.0053[f]
BaBG-5	33.13 ± 4.03[b]	39.93 ± 1.34[b,e]	29.36 ± 1.47[b,f]	24.95 ± 2.01[e,f]	0.082 ± 0.015[b]	0.147 ± 0.0294[b,c,e]	0.088 ± 0.0162[b,f]	0.060 ± 0.0075[e,f,g]
BaBG-10	38.26 ± 4.15[b,c,d]	43.09 ± 5.18[b,c,e]	31.21 ± 3.89[b,e,f]	26.41 ± 3.55[e,f]	0.091 ± 0.025[b]	0.231 ± 0.0336[b,c,d,e]	0.094 ± 0.0102[b,f]	0.062 ± 0.0058[e,f,g]

	(vii) concentration of Si (ppm) in brain			
	D1	D3	D5	D7
control	0.63 ± 0.055	0.59 ± 0.045	0.61 ± 0.058	0.56 ± 0.071
BaBG-1	0.60 ± 0.045	0.71 ± 0.074[b]	0.68 ± 0.126	0.59 ± 0.070[f]
BaBG-5	0.67 ± 0.082	0.80 ± 0.093[b,e]	0.71 ± 0.068[f]	0.62 ± 0.103[f]
BaBG-10	0.63 ± 0.062	0.88 ± 0.120[b,c,e]	0.68 ± 0.053[f]	0.65 ± 0.067[f]

	(viii) concentration of Si (ppm) in lungs			
	D1	D3	D5	D7
control	1.46 ± 0.26	1.62 ± 0.13	1.59 ± 0.22	1.48 ± 0.094
BaBG-1	2.67 ± 0.31[b]	3.38 ± 0.25[b,e]	1.92 ± 0.14[e,f]	1.65 ± 0.23[e,f]
BaBG-5	2.91 ± 0.28[b]	4.04 ± 0.36[b,c,e]	2.17 ± 0.18[b,e,f]	1.73 ± 0.14[e,f,g]
BaBG-10	3.12 ± 0.27[b,c]	4.31 ± 0.52[b,c,e]	2.38 ± 0.31[b,c,e,f]	1.71 ± 0.12[e,f,g]

	(ix) concentration of Si (ppm) in heart			
	D1	D3	D5	D7
control	0.83 ± 0.059	0.92 ± 0.172	0.85 ± 0.390	0.89 ± 0.114
BaBG-1	1.49 ± 0.182[b]	1.78 ± 0.161[b,e]	1.23 ± 0.171[b,f]	0.96 ± 0.083[e,f]
BaBG-5	1.74 ± 0.096[b]	1.96 ± 0.234[b]	1.54 ± 0.201[b,e,f]	1.01 ± 0.160[e,f,g]
BaBG-10	2.05 ± 0.272[b,c,d]	2.15 ± 0.177[b,c]	1.78 ± 0.103[b,e,f]	1.19 ± 0.184[e,f,g]

	(x) concentration of Si (ppm) in liver			
	D1	D3	D5	D7
control	2.08 ± 0.11	2.17 ± 0.34	2.10 ± 0.16	2.02 ± 0.35
BaBG-1	9.19 ± 1.42[b]	14.08 ± 1.31[b,e]	8.44 ± 1.03[b,f]	3.21 ± 0.47[e,f,g]
BaBG-5	12.48 ± 1.78[b,c]	19.16 ± 2.62[b,c,e]	10.61 ± 1.76[b,f]	4.01 ± 0.48[e,f,g]
BaBG-10	17.62 ± 2.49[b,c,d]	24.67 ± 3.26[b,c,d,e]	10.99 ± 2.07[b,c,e,f]	4.96 ± 0.24[b,e,f,g]

	(xi) concentration of Si (ppm) in kidneys			
	D1	D3	D5	D7
control	2.51 ± 0.27	2.98 ± 0.31	2.33 ± 0.20	2.80 ± 0.37
BaBG-1	3.61 ± 0.39[b]	8.21 ± 0.66[b,e]	5.03 ± 0.39[b,e,f]	3.04 ± 0.19[f,g]

https://doi.org/10.1021/acsomega.3c09250
ACS Omega 2024, 9, 7188−7205

http://pubs.acs.org/journal/acsodf

Table 7. continued

(xi)

	concentration of Si (ppm) in kidneys			
	D1	D3	D5	D7
BaBG-5	4.01 ± 0.44^{b}	11.04 ± 1.34^{b,c,e}	6.14 ± 0.48^{b,c,f}	3.97 ± 0.23^{b,f,g}
BaBG-10	6.88 ± 0.71^{b,c,d}	14.27 ± 1.45^{b,c,d,e}	8.88 ± 0.92^{b,c,d,e,f}	4.02 ± 0.46^{b,c,e,f,g}

(xii)

	concentration of Si (ppm) in spleen			
	D1	D3	D5	D7
control	4.71 ± 0.48	4.37 ± 0.30	4.58 ± 0.56	4.19 ± 0.25
BaBG-1	5.42 ± 0.97	9.93 ± 1.64^{b,e}	6.02 ± 0.48^{f}	5.03 ± 0.41^{f}
BaBG-5	7.56 ± 0.53^{b,c}	13.35 ± 1.16^{b,c,e}	8.15 ± 0.97^{b,c,f}	5.89 ± 0.83^{b,e,f,g}
BaBG-10	10.97 ± 1.51^{b,c,d}	17.09 ± 2.31^{b,c,d,e}	10.21 ± 1.35^{b,c,d,f}	6.61 ± 0.39^{b,c,e,f,g}

[a]Data are expressed as mean ± SD (n = 6 male rats/group). $^{b}p < 0.05$, $^{c}p < 0.05$, and $^{d}p < 0.05$ compared to control, 1 mg/kg, and 5 mg/kg BaBG b.w., respectively. $^{e}p < 0.05$, $^{f}p < 0.05$, and $^{g}p < 0.05$ compared to days after the oral treatment of BaBG (D1, D3, and D5 of the individual group, respectively) (two-way ANOVA followed by Bonferroni post hoc test).

to be nontoxic as per the OECD acute and subacute toxicity studies performed on rats.

3.7. *In Vivo* Biodistribution of Ca, Ba, and Si in Vital Organs and Their Scanning Electron Microscopical Analysis. When any inorganic-based biomaterials are designed to be used systemically for therapeutic purposes and have a longer MRT, their organ accumulation and biodistribution in the body are essential parameters that need to be studied. This will help in optimizing the dosage regimen including the route of administration, dose, dosing interval, and the duration of treatment. Biodistribution studies also assist in elucidating the potential organ toxicity or cumulative toxicity that the test compounds might produce. During the *in vivo* pharmacokinetic study, the circulation half-life of Ca, Ba, and Si was found to be 36.85 ± 3.08, 24.71 ± 2.71, and 29.95 ± 3.04 h, respectively (Tables 1−3), at the highest dose tested, thus demonstrating a longer circulation in the body. Hence, the biodistribution of BaBG after oral administration was evaluated in vital organs. As shown in Table 7 and Figure 10, there was a dose-dependent increase in the level of Ca, Ba, and Si in the vital organs (brain, liver, heart, kidneys, lungs, and spleen). At day 1 (D1) post administration of BaBG, there was a statistically significant level of calcium detected in the liver, kidneys, and spleen at a dose of 5 mg/kg compared to the control group. However, at the highest dose, a statistically significant level of Ca was detected in all of the organs compared to the control rats ($p < 0.05$). As time progressed, at D3, the amount detected in all of the organs increased further, and at 10 mg/kg, the increase was almost 1.2-fold compared to D1 (Figure 8). One possible reason may be that after the absorption of leached Ca from BaBG into the systemic circulation, the body tries to maintain homeostasis. There are various physiological calcium stores in the body where the surplus of calcium is stored.[53,54] Additionally, the rapid increase in the Ca level was drastically reduced through urine as a statistically significant amount of Ca was detected in the kidneys (Table 7). In the SEM of the kidney tissue sections of BaBG-treated rats (10 mg/kg), there was the presence of HA (as represented in Figure 10iii). HAs are biocompatible endogenous substances that are biodegradable, and their deposition did not affect the microarchitecture or physiological functioning of kidneys during subacute toxicity study performed in rats.[22] Furthermore, we also observed a higher percentage of Ca accumulation in the spleen compared to that in other organs from D1 along with the deposition of HA (Figure 10ii). The reason may be that the body has normal physiological phenomena to eliminate foreign particles that enter the systemic circulation by phagocytosis into the spleen through the splenic artery. So, either BaBG of smaller size would have been absorbed into the blood from GIT or HA formed *in situ* in the stomach (as observed in the SEM of the stomach tissue in Figure 9) may have migrated to the splenic tissue. Similarly, the liver is also involved in the endocytosis of foreign entities (BaBG) *via* the resident mononuclear macrophages of the RES that are abundantly present.[55] Subsequently, from day 5 onward, the Ca level followed a downhill pattern, and after day 7, we did not find statistically elevated levels of Ca in any of the major organs.

After the dissolution of the glass network, there is simultaneous leaching of Si and Ba in the *in vitro* dissolution study in SBF (Figure 6). Similarly, in the *in vivo* study, there was early detection of these elements in the liver and spleen on D1 (Table 7). Their presence may be due to the opsonization

https://doi.org/10.1021/acsomega.3c09250
ACS Omega 2024, 9, 7188−7205

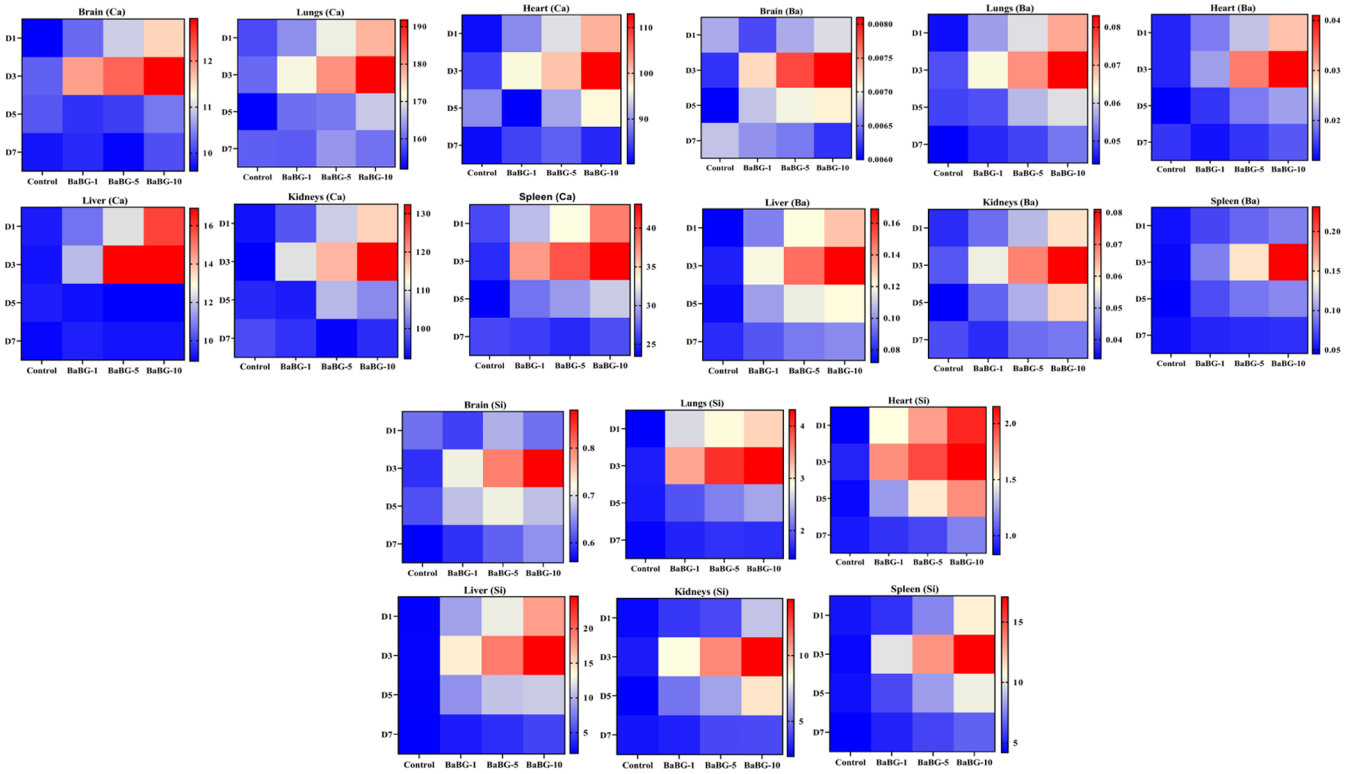

Figure 8. Heatmap representation of the biodistribution of Ca, Ba, and Si in the brain, lungs, heart, liver, kidneys, and spleen of BaBG-treated rats at various doses (1, 5, 10 mg/kg b.w.).

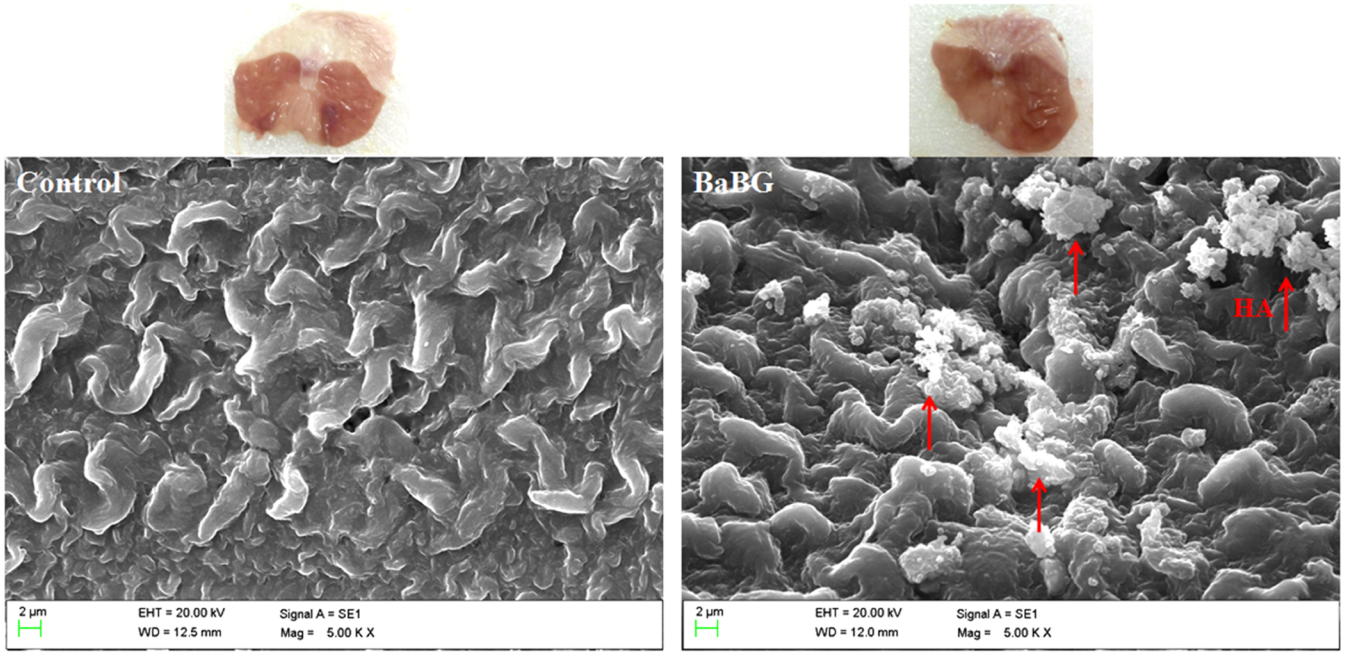

Figure 9. Representative scanning electron microscopy image of the stomach of the control and BaBG-treated rats exhibiting the deposition of abundant hydroxyapatite (HA) crystals on the gastric epithelium layer of the stomach without any abrasion of the protective layer qualitatively. The macroscopic photographs of the stomach of both the groups are also showing normal morphology. Magnification: 5k X; scale bars: 2 μm.

of glass particles by the sinusoidal endothelial cells and Kupffer cells of the liver and phagocytes of the spleen, the major organs for removing the circulating exogenous entities. Statistical analysis by two-way ANOVA exhibited significant elevation in the level of Si and Ba at doses of 5 and 10 mg/kg compared to the control group at D1. Ba increased to 2.53- and 1.28-folds in the spleen and liver, respectively, at the highest dose, while Si was elevated by approximately 1.5-fold in these eliminating organs. A previous study based on the silica-based nanoparticle showed that they were absorbed from the intestine epithelium and are reportedly redistributed mainly in the liver and spleen.[56] Normally, after the oral administration of any

https://doi.org/10.1021/acsomega.3c09250
ACS Omega 2024, 9, 7188−7205

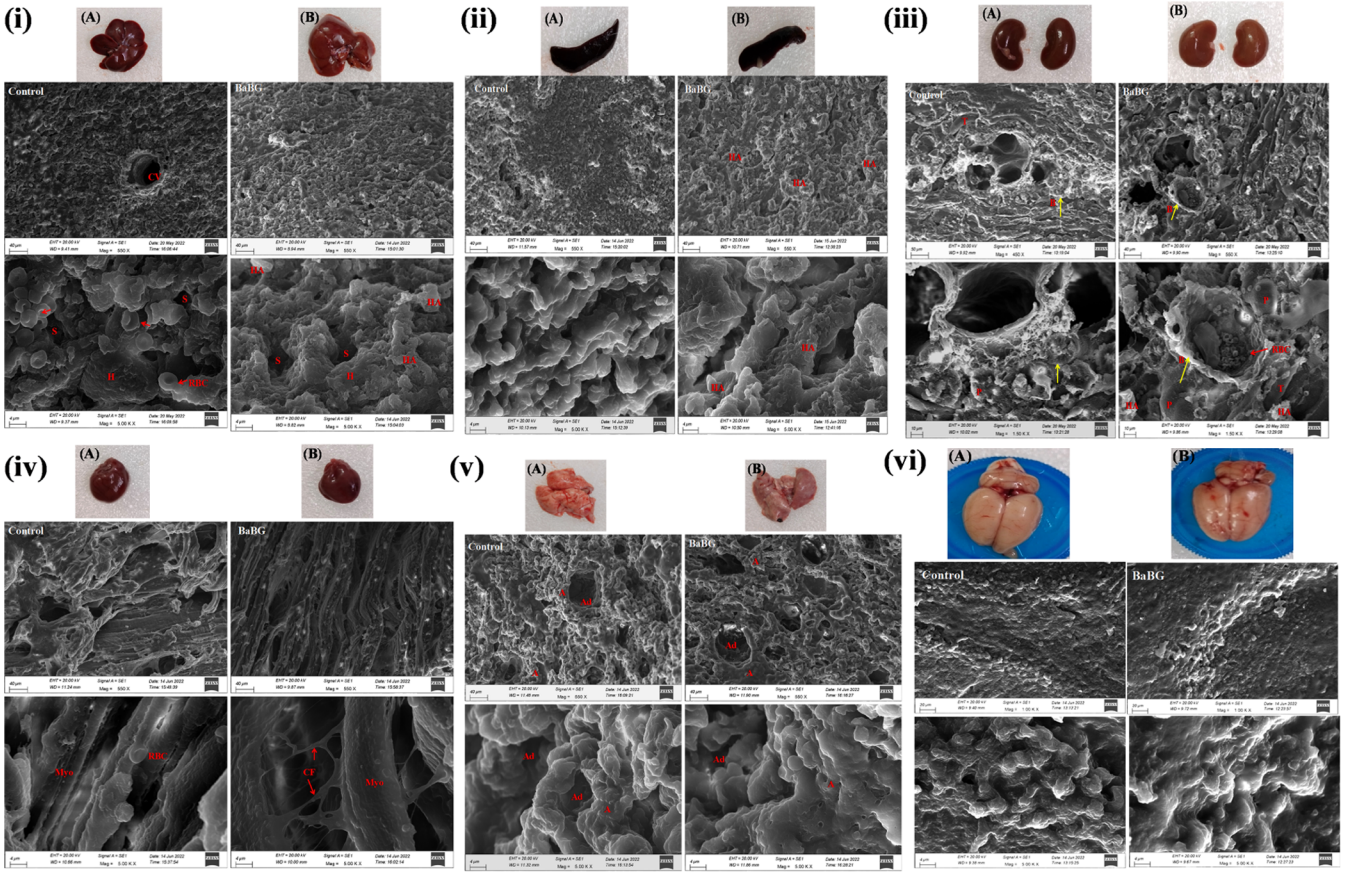

Figure 10. Representative photograph of the scanning electron microscopy of liver (i), spleen (ii), kidney (iii), heart (iv), lungs (v), and brain (vi) sections of control (A) and orally treated BaBG rat (B). The liver section of the treated rat exhibited the presence of normal hepatocytes (H) surrounding the sinusoids (S) and central vein (CV). The deposition of hydroxyapatite (HA) along with the presence of erythrocytes (RBC; shown in red arrow) is seen. The spleen of BaBG-treated rat exhibiting abundant hydroxyapatite (HA) deposition and the lungs of control and BaBG rats also exhibited normal alveoli (A) and alveolar duct (Ad). Similarly, the cross section of the kidneys of the treated rat exhibited a normal architecture of Bowman's capsule (B; yellow arrow) along with the glomerular tuft. There are also podocytes (P) and erythrocytes (RBC) visible along with the deposition of crystals of HA. The SEM analysis of heart exhibited intact myofibers (Myo) with the presence of loose connective tissues and collagen fibers (CF). BaBG rats exhibited a normal surface morphology in the brain section similar to the control rats without any deposition of HA. Magnification of liver, spleen, lung, and heart: 550× and 5k×; scale bars: 40 and 4 μm, respectively. Magnification of kidneys: 450× and 1.5k×; scale bars: 50 and 10 μm, respectively. Magnification of brain: 1k× and 5k×; scale bars: 20 and 4 μm, respectively.

inorganic biomaterials, they are absorbed into the portal vein from the intestine and reach the liver. This could be one possible reason for the presence of HA in the liver (as represented in Figure 10i). Similarly, Ba and Si contents were also elevated significantly in the kidneys from D1 after oral exposure compared to that of the control group. For Si, there was a more than 2-fold increase in its level in the kidneys. On the other hand, Ba and Si were in relatively lower concentration in the brain and lungs (Table 7). The Ba and Si concentrations reached the peak at D3 like Ca in a dose-dependent manner followed by a reduction and leveling off to the basal level. It reflects that there is dose-dependent elevation in the concentration of elements leached from BaBG. Therefore, dose selection should be done cautiously when employing BG for oral or systemic administration during therapeutic intervention.

4. CONCLUSIONS

In the current study, the preclinical single-dose oral release kinetics, biodistribution, and excretion of dopants from sol–gel-derived BaBG were evaluated. BaBG was amorphous and mesoporous in nature, and its bioactivity was affirmed by its ability to form HA in SBF. The *in vitro* release profile for Si, Ca, and Ba from the BaBG framework in the simulated physiological milieu exhibited a controlled release of the dopants with the maximum concentration observed at 24 h for Ca and Si. Similarly, the *in vivo* oral pharmacokinetics study demonstrated a dose-dependent release of network modifiers into the plasma and the T_{max} was observed at 24 h for Si, Ca, and Ba at all doses. There was dose-dependent elevation in the half-life of Si and Ca, and the V_z increased by 4.2- and 4.99-fold, respectively, at 10 mg/kg. However, the half-life for Ba decreased with an increase in dose. The clearance (CL) of Ba increased 1.90- and 3.11-fold at doses 5 and 10 mg/kg, respectively, compared to 1 mg/kg BaBG. Further, the excretion study demonstrated feces to be the prime excretory route for Ba and Si. The biodistribution study indicated that Ca, Ba, and Si accumulated mainly in the excretory organs of the body such as the liver, spleen, and kidneys. Therefore, this study provides information on the fate of the released elements from orally administered BaBG, their release pattern, biodistribution, and excretion.

https://doi.org/10.1021/acsomega.3c09250
ACS Omega 2024, 9, 7188−7205

■ ASSOCIATED CONTENT

Supporting Information

The Supporting Information is available free of charge at https://pubs.acs.org/doi/10.1021/acsomega.3c09250.

Nitrogen adsorption−desorption isotherm of BaBG; the XRD pattern of BaBG before and after SBF treatment for 7 days; the particle size distribution of BaBG; effect of oral administration of BaBG on body weight (i) and organ coefficient of the heart (ii), brain (iii), lungs (iv), liver (v), kidneys (vi), and spleen (vii) of rats at various time intervals; all values are in mean ± SD (n = 6 male rats/group) (two-way ANOVA followed by Bonferroni post hoc test) (PDF)

■ AUTHOR INFORMATION

Corresponding Author

Sairam Krishnamurthy − *Neurotherapeutics Laboratory, Department of Pharmaceutical Engineering and Technology, Indian Institute of Technology (Banaras Hindu University), Varanasi 221005, India;* orcid.org/0000-0003-4159-2463; Email: ksairam.phe@iitbhu.ac.in

Authors

Shreyasi Majumdar − *Neurotherapeutics Laboratory, Department of Pharmaceutical Engineering and Technology, Indian Institute of Technology (Banaras Hindu University), Varanasi 221005, India*

Anshul Tiwari − *Analytical Sciences and Accredited Testing Services, CSIR-Indian Institute of Toxicology Research, Lucknow 226001, India*

Debasmit Mallick − *Department of Zoology, Institute of Science, Banaras Hindu University, Varanasi 221005, India*

Devendra K. Patel − *Analytical Sciences and Accredited Testing Services, CSIR-Indian Institute of Toxicology Research, Lucknow 226001, India;* orcid.org/0000-0002-0168-9132

Surendra Kumar Trigun − *Department of Zoology, Institute of Science, Banaras Hindu University, Varanasi 221005, India*

Complete contact information is available at: https://pubs.acs.org/10.1021/acsomega.3c09250

Author Contributions

S.M.: experimentation, data collection, data analysis, manuscript writing, and editing. A.T. and D.K.P.: ICP-MS facility and data collection. D.M. and S.K.T.: SEM facility and data collection. S.K.: conceptualization, data analysis, reviewing, and editing the manuscript.

Funding

S.M. received financial assistance from the Department of Science and Technology (DST) through the INSPIRE Fellowship [Grant no. DST/INSPIRE Fellowship/IF180166].

Notes

The authors declare no competing financial interest.

■ ACKNOWLEDGMENTS

The authors wish to acknowledge the Central Instrument Facility, Zoology Department, Banaras Hindu University (BHU), Varanasi, India, for the SEM facility used in this research work.

■ REFERENCES

(1) Majumdar, S.; Gupta, S.; Krishnamurthy, S.Bioactive Glass: Soft Tissue Reparative and Regenerative Applications. In *Bioactive Glasses and Glass-Ceramics: Fundamentals and Applications*; Wiley, 2022; pp 479−517.

(2) Taye, M. B. Biomedical applications of ion-doped bioactive glass: A review. *Appl. Nanosci.* **2022**, *12* (12), 3797−3812.

(3) Majumdar, S.; Gupta, S.; Krishnamurthy, S. Multifarious applications of bioactive glasses in soft tissue engineering. *Biomater. Sci.* **2021**, *9* (24), 8111−8147.

(4) Chen, Q.; Wu, J.; Liu, Y.; Li, Y.; Zhang, C.; Qi, W.; Yeung, K. W.; Wong, T. M.; Zhao, X.; Pan, H. Electrospun chitosan/PVA/bioglass Nanofibrous membrane with spatially designed structure for accelerating chronic wound healing. *Mater. Sci. Eng., C* **2019**, *105*, No. 110083.

(5) Qi, Q.; Zhu, Y.; Liu, G.; Yuan, Z.; Li, H.; Zhao, Q. Local intramyocardial delivery of bioglass with alginate hydrogels for post-infarct myocardial regeneration. *Biomed. Pharmacother.* **2020**, *129*, No. 110382.

(6) Paliwal, P.; Kumar, A. S.; Tripathi, H.; Singh, S. P.; Patne, S. C.; Krishnamurthy, S. Pharmacological application of barium containing bioactive glass in gastro-duodenal ulcers. *Mater. Sci. Eng., C* **2018**, *92*, 424−434.

(7) Cohen, S. M. New approaches for medicinal applications of bioinorganic chemistry. *Curr. Opin. Chem. Biol.* **2007**, *11* (2), 115−120.

(8) Gupta, S.; Majumdar, S.; Krishnamurthy, S. Bioactive glass: A multifunctional delivery system. *J. Controlled Release* **2021**, *335*, 481−497.

(9) Schepers, E. J.; Ducheyne, P.; Barbier, L.; Schepers, S. Bioactive glass particles of narrow size range: a new material for the repair of bone defects. *Implant Dent.* **1993**, *2* (3), 151−157.

(10) Jones, J. R.; Brauer, D. S.; Hupa, L.; Greenspan, D. C. Bioglass and bioactive glasses and their impact on healthcare. *Int. J. Appl. Glass Sci.* **2016**, *7* (4), 423−434.

(11) Rivadeneira, J.; Luz, G. M.; Audisio, M. C.; Mano, J. F.; Gorustovich, A. A. Novel antibacterial bioactive glass nanocomposite functionalized with tetracycline hydrochloride. *Biomed. Glasses* **2015**, *1* (1), 128−135, DOI: 10.1515/bglass-2015-0012.

(12) Zheng, K.; Kapp, M.; Boccaccini, A. R. Protein interactions with bioactive glass surfaces: a review. *Appl. Materi. Today* **2019**, *15*, 350−371.

(13) Akula, P.; PK, L. Effect of pH on weakly acidic and basic model drugs and determination of their ex vivo transdermal permeation routes. *Braz. J. Pharm. Sci.* **2018**, *54*, No. e00070, DOI: 10.1590/s2175-97902018000200070.

(14) Mao, C.; Chen, X.; Hu, Q.; Miao, G.; Lin, C. Acute toxicity and in vivo biodistribution of monodispersed mesoporous bioactive glass spheres in intravenously exposed mice. *Mater. Sci. Eng., C* **2016**, *58*, 682−691.

(15) Schwartz, S.; Pateman, T. Pre-clinical Pharmacokinetics. In *A Handbook of Bioanalysis and Drug Metabolism*; CRC Press, 2021; pp 113−131.

(16) Hench, L. L. The story of Bioglass. *J. Mater. Sci.: Mater. Med.* **2006**, *17* (11), 967−978.

(17) Schroeder, H. A.; Tipton, I. H.; Nason, A. P. Trace metals in man: strontium and barium. *J. Chronic Dis.* **1972**, *25* (9), 491−517.

(18) Moore, W., Jr. Comparative metabolism of barium-133 and calcium-45 by embryonic bone grown in vitro. *Radiat. Res.* **1964**, *21* (3), 376−382.

(19) Madanat, R.; Moritz, N.; Vedel, E.; Svedström, E.; Aro, H. T. Radio-opaque bioactive glass markers for radiostereometric analysis. *Acta Biomater.* **2009**, *5* (9), 3497−3505.

(20) Majumdar, S.; Hira, S. K.; Tripathi, H.; Kumar, A. S.; Manna, P. P.; Singh, S.; Krishnamurthy, S. Synthesis and characterization of barium-doped bioactive glass with potential anti-inflammatory activity. *Ceram. Int.* **2021**, *47* (5), 7143−7158.

(21) Satoh, S.; Kubota, Y.; Itoh, T.; Kuriyama, H. Mechanisms of the Ba2+-induced contraction in smooth muscle cells of the rabbit mesenteric artery. *J. Gen. Physiol.* **1987**, *89* (2), 215−237.
(22) Majumdar, S.; Krishnamurthy, S. In vivo toxicological evaluation of barium-doped bioactive glass in rats. *Ceram. Int.* **2022**, *48* (22), 33288−33305.
(23) Kokubo, T.; Takadama, H. How useful is SBF in predicting in vivo bone bioactivity? *Biomaterials* **2006**, *27* (15), 2907−2915.
(24) Balbinot, G. d. S.; Leitune, V. C. B.; Nunes, J. S.; Visioli, F.; Collares, F. M. Synthesis of sol−gel derived calcium silicate particles and development of a bioactive endodontic cement. *Dent. Mater.* **2020**, *36* (1), 135−144.
(25) Macon, A. L. B.; Kim, T. B.; Valliant, E. M.; Goetschius, K.; Brow, R. K.; Day, D. E.; Hoppe, A.; Boccaccini, A. R.; Kim, I. Y.; Ohtsuki, C. A unified in vitro evaluation for apatite-forming ability of bioactive glasses and their variants. *J. Mater. Sci.: Mater. Med.* **2015**, *26*, No. 115.
(26) Prajapati, S. K.; Krishnamurthy, S. Development and treatment of cognitive inflexibility in sub-chronic stress−re-stress (SRS) model of PTSD. *Pharmacol. Rep.* **2021**, *73*, 464−479.
(27) Zhang, Y.; Huo, M.; Zhou, J.; Xie, S. PKSolver: An add-in program for pharmacokinetic and pharmacodynamic data analysis in Microsoft Excel. *Comput. Methods Programs Biomed.* **2010**, *99* (3), 306−314.
(28) Dumala, N.; Mangalampalli, B.; Kalyan Kamal, S. S.; Grover, P. Repeated oral dose toxicity study of nickel oxide nanoparticles in Wistar rats: a histological and biochemical perspective. *J. Appl. Toxicol.* **2019**, *39* (7), 1012−1029.
(29) Mukhtar, A.; Mellon, N.; Saqib, S.; Lee, S.-P.; Bustam, M. A. Extension of BET theory to CO 2 adsorption isotherms for ultra-microporosity of covalent organic polymers. *SN Appl. Sci.* **2020**, *2*, No. 1232.
(30) Shi, C.; Hou, X.; Zhao, D.; Wang, H.; Guo, R.; Zhou, Y. Preparation of the bioglass/chitosan-alginate composite scaffolds with high bioactivity and mechanical properties as bone graft materials. *J. Mech. Behav. Biomed. Mater.* **2022**, *126*, No. 105062.
(31) Arruebo, M. Drug delivery from structured porous inorganic materials. *Wiley Interdiscip. Rev.: Nanomed. Nanobiotechnol.* **2012**, *4* (1), 16−30.
(32) Fiume, E.; Migneco, C.; Verné, E.; Baino, F. Comparison between Bioactive Sol-Gel and Melt-Derived Glasses/Glass-Ceramics Based on the Multicomponent SiO2−P2O5−CaO−MgO−Na2O−K2O System. *Materials* **2020**, *13* (3), 540.
(33) Kokubo, T.; Kushitani, H.; Sakka, S.; Kitsugi, T.; Yamamuro, T. Solutions able to reproduce in vivo surface-structure changes in bioactive glass-ceramic A-W3. *J. Biomed. Mater. Res.* **1990**, *24* (6), 721−734.
(34) Kattimani, V. S.; Kondaka, S.; Lingamaneni, K. P. Hydroxyapatite−-Past, present, and future in bone regeneration. *Bone Tissue Regener. Insights* **2016**, *7*, No. BTRI.S36138.
(35) Sopcak, T.; Shepa, I.; Csanádi, T.; Medvecky, L.; Giretova, M.; Kucharova, V.; Sedlak, R.; Balazsi, K.; Stulajterova, R.; Streckova, M. Influence of boron addition on the phase transformation, microstructure, mechanical and in-vitro cellular properties of bredigite-type coatings deposited by a spin coating technique. *Mater. Chem. Phys.* **2022**, *283*, No. 126049.
(36) Mozafari, M.; Banijamali, S.; Baino, F.; Kargozar, S.; Hill, R. G. Calcium carbonate: Adored and ignored in bioactivity assessment. *Acta Biomater.* **2019**, *91*, 35−47.
(37) De Oliveira, A. A. R.; De Souza, D. A.; Dias, L. L. S.; De Carvalho, S. M.; Mansur, H. S.; de Magalhaes Pereira, M. Synthesis, characterization and cytocompatibility of spherical bioactive glass nanoparticles for potential hard tissue engineering applications. *Biomed. Mater.* **2013**, *8* (2), No. 025011.
(38) Yadav, S.; Singh, P.; Pyare, R. Synthesis, characterization, mechanical and biological properties of biocomposite based on zirconia containing 1393 bioactive glass with hydroxyapatite. *Ceram. Int.* **2020**, *46* (8), 10442−10451.
(39) Arcos, D.; Greenspan, D.; Vallet-Regi, M. Influence of the Stabilization Temperature on Textural and Structural Features and Ion Release in SiO2− CaO− P2O5 Sol− Gel Glasses. *Chem. Mater.* **2002**, *14* (4), 1515−1522.
(40) Wanner, M.; Walker, W.; Sutter, H. M.; Riond, J. L.; Broz, J. Influence of dietary citric acid and calcium on the bioavailability of orally administered chlortetracycline in piglets. *J. Vet. Med., Ser. A* **1991**, *38* (1−10), 755−762.
(41) Kim, K. J.; Kim, M. S.; Hong, N.; Bae, J. H.; Kim, K. J.; Kim, N. H.; Rhee, Y.; Lee, J.; Kim, S. G. Cardiovascular risks associated with calcium supplementation in patients with osteoporosis: a nationwide cohort study. *Eur. Heart J.: Cardiovasc. Pharmacother.* **2022**, *8* (6), 568−577.
(42) Bligh, P.; Taylor, D. Comparative studies of the metabolism of strontium and barium in the rat. *Biochem. J.* **1963**, *87* (3), 612.
(43) Matikainen, N.; Pekkarinen, T.; Ryhänen, E. M.; Schalin-Jäntti, C. Physiology of calcium homeostasis: an overview. *Endocrinol. Metab. Clin. North Am.* **2021**, *50* (4), 575−590.
(44) Kovrlija, I.; Locs, J.; Loca, D. Incorporation of barium ions into biomaterials: dangerous liaison or potential revolution? *Materials* **2021**, *14* (19), 5772.
(45) Kravchenko, J.; Darrah, T. H.; Miller, R. K.; Lyerly, H. K.; Vengosh, A. A review of the health impacts of barium from natural and anthropogenic exposure. *Environ. Geochem. Health* **2014**, *36*, 797−814.
(46) Du, Z.; Chen, S.; Cui, G.; Yang, Y.; Zhang, E.; Wang, Q.; Lavin, M. F.; Yeo, A. J.; Bo, C.; Zhang, Y. Silica nanoparticles induce cardiomyocyte apoptosis via the mitochondrial pathway in rats following intratracheal instillation. *Int. J. Mol. Med.* **2019**, *43* (3), 1229−1240.
(47) Lee, J.-A.; Kim, M.-K.; Paek, H.-J.; Kim, Y.-R.; Kim, M.-K.; Lee, J.-K.; Jeong, J.; Choi, S.-J. Tissue distribution and excretion kinetics of orally administered silica nanoparticles in rats. *Int. J. Nanomed.* **2014**, *9* (Suppl 2), 251−260.
(48) Blaine, J.; Chonchol, M.; Levi, M. Renal control of calcium, phosphate, and magnesium homeostasis. *Clin. J. Am. Soc. Nephrol.* **2015**, *10* (7), 1257.
(49) Panahifar, A.; Chapman, L. D.; Weber, L.; Samadi, N.; Cooper, D. M. Biodistribution of strontium and barium in the developing and mature skeleton of rats. *J. Bone Miner. Metab.* **2019**, *37*, 385−398.
(50) Ross, A.; Taylor, C.; Yaktine, A.; Valle, H. Overview of calcium—dietary reference intakes for calcium and vitamin D—NCBI bookshelf. *Pediatrics* **2012**, *130* (1427), 10.1542.
(51) Moffett, D.; Smith-Simon, C.; Stevens, Y.-W. *Toxicological Profile for Barium and Barium Compounds*, 2007.
(52) Stoewsand, G.; Anderson, J.; Rutzke, M.; Lisk, D. Deposition of barium in the skeleton of rats fed Brazil nuts. *Nutr. Rep. Int.* **1988**, *38* (2), 259−262.
(53) Cheng, H.; Wei, S.; Wei, L.; Verkhratsky, A. *Calcium Signaling in Physiology and Pathophysiology*; Wiley Online Library, 2006; Vol. *27*, pp 767−772.
(54) Patel, S.; Docampo, R. Acidic calcium stores open for business: expanding the potential for intracellular Ca2+ signaling. *Trends Cell Biol.* **2010**, *20* (5), 277−286.
(55) Bhandari, S.; Larsen, A. K.; McCourt, P.; Smedsrød, B.; Sørensen, K. K. The scavenger function of liver sinusoidal endothelial cells in health and disease. *Front. Physiol.* **2021**, *12*, No. 757469.
(56) Fu, C.; Liu, T.; Li, L.; Liu, H.; Chen, D.; Tang, F. The absorption, distribution, excretion and toxicity of mesoporous silica nanoparticles in mice following different exposure routes. *Biomaterials* **2013**, *34* (10), 2565−2575.

https://doi.org/10.1021/acsomega.3c09250
ACS Omega 2024, 9, 7188−7205